SARS-CoV-2 invades cognitive centers of the brain and induces Alzheimer's-like neuropathology

Wei-Bin Shen[1#], Montasir Elahi[1#], James Logue[2#], Penghua Yang[1], Lauren Baracco[2], E. Albert Reece[1, 3], Bingbing Wang[1], Ling Li[4], Thomas G Blanchard[4], Zhe Han[5], Robert A Rissman[6, 7], Matthew B Frieman[2], Peixin Yang[1, 3 *]

[1]Department of Obstetrics, Gynecology & Reproductive Sciences, University of Maryland School of Medicine, Baltimore, Maryland, USA.
[2] Department of Microbiology and Immunology, University of Maryland School of Medicine, Baltimore, MD 21201, USA.
[3]Department of Biochemistry & Molecular Biology, University of Maryland School of Medicine, Baltimore, Maryland, USA.
[4]Department of Pediatrics, University of Maryland School of Medicine, Baltimore, MD, USA.
[5]Department of Medicine, University of Maryland School of Medicine, Baltimore, MD, USA.
[6]Department of Neurosciences, University of California San Diego, La Jolla, CA, 92093.
[7]Shiley-Marcos Alzheimer's Disease Research Center, University of California San Diego, La Jolla, California, 92093.
[#] These authors contributed equally to this work.
*Correspondence: Peixin Yang, PhD, Department of Obstetrics, Gynecology & Reproductive Sciences, University of Maryland School of Medicine, BRB11-039, 655 W. Baltimore Street, Baltimore, MD, 21201. Email: pyang@som.umaryland.edu, Tel: 410-706-8402, Fax: 410-706-5747. Matthew B Frieman, PhD, Department of Microbiology and Immunology, University of Maryland School of Medicine, Baltimore, MD 21201, USA. Email: mfrieman@som.umaryland.edu

Conflict of interest statement: The authors have declared that no conflict of interest exists
Subheading: Neurodegenerative phenotypes in COVID-19

Keywords: SARS-CoV-2; degenerating neurons; iPSC; Alzheimer's disease; COVID-19 brains; Alzheimer's infectious etiology; Abeta aggregation; p-tau aggregation; activated microglia; neuroinflammation; tauopathy.

Abstract

The neurotropism of SARS-CoV-2 and the phenotypes of infected neurons are still in debate. Long COVID manifests with "brain diseases" and the cause of these brain dysfunction is mysterious. Here, we analyze 34 age- and underlying disease-matched COVID-19 or non-COVID-19 human brains. SARS-CoV-2 RNA, nucleocapsid, and spike proteins are present in neurons of the cognitive centers of all COVID-19 patients, with its non-structural protein NSF2 detected in adult cases but not in the infant case, indicating viral replications in mature neurons. In adult COVID-19 patients without underlying neurodegeneration, SARS-CoV-2 infection triggers Aβ and p-tau deposition, degenerating neurons, microglia activation, and increased cytokine, in some cases with Aβ plaques and p-tau pretangles. The number of SARS-CoV-2^{+} cells is higher in patients with neurodegenerative diseases than in those without such conditions. SARS-CoV-2 further activates microglia and induces Aβ and p-tau deposits in non-Alzheimer's neurodegenerative disease patients. SARS-CoV-2 infects mature neurons derived from inducible pluripotent stem cells from healthy and Alzheimer's disease (AD) individuals through its receptor ACE2 and facilitator neuropilin-1. SARS-CoV-2 triggers AD-like gene programs in healthy neurons and exacerbates AD neuropathology. An AD infectious etiology gene signature is identified through SARS-CoV-2 infection and silencing the top three downregulated genes in human primary neurons recapitulates the neurodegenerative phenotypes of SARS-CoV-2. Thus, our data suggest that SARS-CoV-2 invades the brain and activates an AD-like program.

Introduction

The COVID-19 pandemic caused by severe acute respiratory syndrome coronavirus 2 (SARS-CoV-2) has infected at least 570 million people worldwide and 90.3 million Americans to date. SARS-CoV-2 not only causes respiratory syndromes but also leads to neurological abnormalities, with an 85% occurrence rate in patients with Alzheimer's disease (AD) [1,2]. In fact, neurological symptoms, including hypogeusia, headache, and anosmia, precede the onset of respiratory symptoms in the majority of patients with COVID-19. The major chronic sequelae of COVID-19 are expected to be cognitive decline and dementia [3]. A recent study has shown that one-third of COVID-19 survivors exhibit substantial neurological and psychiatric morbidity in the 6 months after SARS-CoV-2 infection [4]. Furthermore, the "brain disease" risk is not limited to patients who have severe COVID-19 [4]. Thus, the COVID-19 pandemic provides a unique but unwelcomed opportunity to study the contribution of SARS-CoV-2 to neurological disorders, including AD.

It has been proposed that β-coronaviruses, including SARS-CoV-2, can invade the central nervous system [5]. The two coronaviruses closely related to SARS-CoV-2, Middle Eastern respiratory syndrome coronavirus (MERS-CoV) and severe acute respiratory syndrome coronavirus 1 (SARS-CoV-1), can infect the central nervous system [6,7]. A recent study shows the presence of SARS-CoV-2 in a patient's olfactory mucosa and its neuronal projections [8]. SARS-CoV-2 RNA is present in 36.4% of brain biopsies of fatal COVID-19 cases [9]. A recent study observes the presence of SARS-CoV-2 spike protein in some brain regions in all three COVID-19 cases studied [10]. In transgenic hACE2 mice, SARS-CoV-2 is massively present in the brain on post-infection day 5 [11]. In addition to the olfactory transmucosal entry of SARS-CoV-2 into the central nervous system (CNS) [8], other potential routes of SARS-CoV-2 brain entry, including blood-brain barrier (BBB) passage, especially under conditions of a compromised BBB, such as in cases of AD and autism [12,13], and the infiltration of infected immune cells have been proposed

[14], though evidence for infected immune cells remains scarce. However, neurological disorders are not limited to severe COVID-19 cases, suggesting that multiple brain entries may account for SARS-CoV-2 neurotropism. Although SARS-CoV-2 can enter the brain, experimental evidence of its presence in key brain regions involved in cognitive functions is still lacking, and little is known about the functional impact of SARS-CoV-2 CNS invasion on neurons.

SARS-CoV-2 entry into host cells is facilitated by its cell surface receptors. The spike proteins of both SARS-CoV-2 and the earlier SARS-CoV-1 bind to angiotensin-converting enzyme 2 (ACE2) as the first step of cellular entry [15]. The presence of ACE2 in neurons of the brain has been demonstrated [16]. However, ACE2 is expressed at relatively low levels in most tissues [17]. SARS-CoV-2 exhibits much higher infectivity than SARS-CoV-1. This evidence implicates either the existence of other cell surface receptors in SARS-CoV-2 cell entry or the facilitation of cell entry by other factors. Indeed, neuropilin-1 (NRP1) has been identified as a facilitator of SARS-CoV-2 entry when ACE2 is expressed, leading to high rates of infection [17]. NRP1 effectively binds to the protease furin-cleaved spike protein of SARS-CoV-2 [17], a process that does not occur for SARS-CoV-1. NRP1 is abundantly expressed in cells of many tissues including neurons [18]. The presence of ACE2 and NRP1 in neurons suggests the high possibility of neurotropism. It is of interest to determine in which cell types in the CNS and at which stage of neural development SARS-CoV-2 can exert its infectibility.

There is a suggested link between SARS-CoV-2 infection and dementia/AD. The 2002 and 2012 SARS and MERS epidemics caused memory impairment in many recovered patients [19]. Neurological syndromes related to AD, including neuroinflammatory syndromes [20,21], seizures [22], delirium [23,24], and alterations in personality, behavior, and cognitive deficits [20,25], frequently occur in patients with COVID-19 who recover from COVID-19. Thus, SARS-CoV-2 infection of the brain may increase the risk of AD. The direct effects of SARS-CoV-2 on neuronal function and survival, the inflammatory cytokine response,

and hypoxia may lead to an Alzheimer's-like manifestation [26,27]. Additionally, AD patients have twice the risk of contracting COVID-19, which deteriorates AD symptoms and increases mortality [28]. The cellular mechanism underlying the possible neurotropism of SARS-CoV-2 needs to be revealed for the development of possible treatments for many COVID-19 survivors suffering from neurological disorders.

In this study, we sought to test whether SARS-CoV-2 is neurotropic and infects neurons in the cognitive centers of 34 COVID-19 or non-COVID-19 cases with or without neurodegenerative diseases. We have found that SARS-CoV-2 invades the cognitive centers of all 17 COVID-19 patients with a greater degree in neurodegenerative disease patients, induces AD-like neuropathology in non-neurodegenerative disease brains, and enhances neuroinflammation in neurodegenerative disease patients. SARS-CoV-2 infects human inducible pluripotent stem cell (iPSC)-derived mature neurons from healthy individuals, leading to amyloid beta (Aβ) deposition, increased inflammation, neuronal death, and increased expression of AD mediators. Strikingly, we found that SARS-CoV-2-infects neurons from healthy individuals through a shared gene expression program with non-infected AD neurons, leading to activation of the infectious pathways and supporting the infectious etiology of AD.

Results

SARS-CoV-2 invades cognitive centers of the brain

Because ACE2, the SARS-CoV-2 cellular receptor, and NRP1, a facilitator of SARS-CoV-2 entry, are expressed in CNS neurons, we hypothesized that SARS-CoV-2 can infect neurons in the brain, especially with underlying conditions such as Alzheimer's disease (AD) and other neurodegenerative diseases. We sought to determine whether SARS-CoV-2 invades the cognitive centers of the brain.

The 17 COVID-19 cases were matched to 17 non-COVID-19 cases by age, underlying diseases, postmortem intervals, retrieval time window, and other parameters when it is possible (Supplementary Table 1). RNAscope *in situ* hybridization detected SARS-CoV-2 RNA in all 17 COVID-19 cases but not in the 17 matched non-COVID-19 cases, in the three cortical regions, the entorhinal (ENT) cortex, the inferior frontal cortex (IPC) and the dorsolateral prefrontal cortex (DPC) (Fig. 1A, Supplementary Fig. 1A). The ENT had the highest signal among the three cortexes (Fig. 1A). The SARS-CoV-2 RNA signals in the five COVID-19 cases with neurodegenerative diseases (ND) including AD, dementia, frontotemporal dementia (FTD), Lewy Body Dementia (LBD) and progressive supranuclear palsy (PSP), were higher than those in the twelve COVID-19 cases without neurodegenerative diseases (Fig. 1B). PCR analysis using the CDC method[29] confirmed the presence of SARS-CoV-2 RNA in the three cases that had frozen brain tissues (Supplementary Fig. 1B). In the 31-year-old COVID-19 non-neurodegenerative disease (NND) case (6436), the amounts of SARS-CoV-2 RNA in the ENT and the IPC were comparable to those in the lungs (Supplementary Fig. 1B). In the COVID-19 NND case (5922) and the COVID-19 without any underlying conditions (5922), SARS-CoV-2 RNA was also detected, whereas there was no SARS-CoV-2 RNA in the age-matched non-COVID-19 ND (6207) individual or in the age-matched non-COVID-19 apparently healthy individual (6168) (Supplementary Fig. 1B).

The SARS-CoV-2 nucleocapsid protein (N) and spike (S) protein were present in the entorhinal

cortex of the 17 COVID-19 cases, with a negligible amount of these two proteins in the infant case (#3177) (Fig. 1C, Supplementary Fig. 1C, D). The entorhinal cortex had the highest amount of N and S proteins compared to the other two cortex IPC and DPC (Fig. 1 D, Supplementary Fig. 1D). The amount of N and S proteins in the five COVID-19 cases with neurodegenerative diseases was higher than that in the twelve COVID-19 cases without neurodegenerative diseases (Fig. 1D, Supplementary Fig. 1D). In contrast, there was no positive staining of spike protein or nucleocapsid (N) protein in the cortical regions of the matched non-COVID-19 cases (Fig. 1C, Supplementary Fig. 1C, D).

ACE2 positive neurons show SARS-CoV-2 positivity and neurodegeneration

Because SARS-CoV-2 exists in cortical cells in COVID-19 patients, these cells must express ACE2. In the entorhinal cortex of adult COVID-19 cases, ACE2 co-localized with the mature neuron marker MAP2 in the periphery of neurons (Fig. 2A, Supplementary Fig. 2A), whereas in the infant case, ACE2 was not present in neurons and only a few neurons were labeled by MAP2 (Fig. 2A). The blood vessels in the brain had a robust ACE2 expression; however, ACE2 expression in neuronal cells was relatively low (Fig. 2A). ACE2 positive cells in the entorhinal cortex of COVID-19 cases were also N protein positive (Fig. 2C), indicating SARS-CoV-2 infects neurons through its receptor ACE2.

Next, we sought to determine whether cortical neurons were infected by SARS-CoV-2 with the potential of replication in these cells. Indeed, the SARS-CoV-2 RNA co-localized with the neuron marker NeuN in both the infant and adult COVID-19 cases but was absent in NeuN positive cells of non-COVID-19 cases (Fig. 2D, Supplementary Fig. 2B). Likewise, the S protein was present in the NeuN positive cells of adult COVID-19 cases but not in those of non-COVID-19 cases (Fig. 2E, Supplementary Fig. 2C). To assess whether SARS-CoV-2 replicates in neurons, we detected the SARS-CoV-2 non-structural protein NSP2. NSP2 was present in cells of the adult COVID-19 cases but not in cells of the infant COVID-19 case (Fig. 2F), suggesting that SARS-CoV-2 replicates in the brain of adult COVID-19 patients.

To determine whether SARS-CoV-2-infected neurons show neurodegenerative phenotypes, we used the Fluoro-Jade C to label degenerating neurons[30,31]. Fluoro-Jade C was co-labeled with either the N protein or the S protein in the entorhinal cortex of adult COVID-19 cases without neurodegenerative diseases (Fig. 2G, Supplementary Fig. 2D). Fluoro-Jade C positive degenerating neurons were not detected in the entorhinal cortex of adult non-COVID-19 cases without neurodegenerative diseases (Fig. 2G, Supplementary Fig. 2D). There were no significant but slightly higher numbers of degenerating neurons between the COVID-19 and the non-COVID-19 individuals with neurodegenerative diseases (Fig. 2G). These results suggest that SARS-CoV-2-infected neurons are undergoing neurodegeneration.

SARS-CoV-2 induces AD-like neuropathological phenotypes

To further characterize the neurodegenerative phenotypes of SARS-CoV-2-infected neurons, we focused on the two AD preclinical markers, cellular Aβ (amyloid beta) and phospho-tau (microtubule-associated protein tau). Cellular Aβ aggregates were observed in the entorhinal cortex of the eleven adult COVID-19 cases without neurodegenerative diseases but not in the infant COVID-19 case (Fig. 3A), whereas it was not present in the cortex of age-matched non-COVID-19 cases (Fig. 3A, Supplementary Fig. 3A). Cellular Aβ aggregations and extracellular Aβ plaques were observed in the FTD, Dementia, LBD and the PSP cases infected with COVID-19 but not in the age and disease type-matched controls (Fig. 3A, Supplementary Fig. 3A). Immunofluorescence analysis with thioflavin-T confirmed that the cytoplasmic deposition of Aβ in the COVID-19 cases consisted of aggregated Aβ (Fig. 3B). Aβ aggregations and plaques were also observed in the IPC and the DPC of adult COVID-19 cases without neurodegenerative diseases (Fig. 3C).

One of the preclinical hallmarks of AD is the intracellular deposit of hyperphosphorylated tau, which is associated with neuronal dysfunction, cognitive deficit, and neuronal death [32,33]. p-tau at serine 202 aggregations were detected in the entorhinal cortex of the eleven adult COVID-19 cases without

neurodegenerative diseases but not in the infant COVID-19 case (Fig. 3D), and there was no p-tau detected in the age- and disease type-matched controls (Fig. 3D, Supplementary Fig. 3B). In the FTD and the LBD COVID-19 cases, intracellular deposit of p-tau were detected, whereas non-COVID-19 LBD, FTD did not show intracellular p-tau deposit (Fig. 3D, Supplementary Fig. 3B). In adult COVID-19 NND brains, p-tau were primarily present in N protein positive cells (Fig. 3E, Supplementary Fig. 3C). p-tau deposits were also present in the IPC and the DPC, with the ENT having the most (Fig. 3F). Thus, SARS-CoV-2 infection might link to AD neuropathology.

SARS-CoV-2 induces neuroinflammation

It has been suggested that SARS-CoV-2 infection leads to neuroinflammation. However, direct evidence on the link between SARS-CoV-2 and neuroinflammation is still lacking. Activated microglia was induced in all COVID-19 cases without neurodegenerative diseases (Fig. 4A). In contrast, the microglia were at their resting stages in the entorhinal cortex of age-matched non-COVID-19 cases (Fig. 4A, Supplementary Fig. 4A). The number of activated microglia was higher in the entorhinal cortexes of COVID-19 cases with neurodegenerative diseases than those of non-COVID-19 cases with neurodegenerative diseases (Fig. 4A, B, Supplementary Fig. 4A).

The protein expression of two cytokines, IL-6 (interleukin 6) and IL-1β, was significantly increased in the entorhinal cortex of adult COVID-19 cases without neurodegenerative diseases, compared to their respective non-COVID-19 controls (Fig. 4C, D, Supplementary Fig. 4B, C). The number of IL-6 and IL-1β positive cells in the COVID-19 cases with neurodegenerative diseases was higher than that in non-COVID-19 cases with neurodegenerative diseases (Fig. 4C, D, Supplementary Fig. 4B, C). This evidence collectively suggested that SARS-CoV-2 infection further enhances neuroinflammation in neurodegenerative disease patients.

SARS-CoV-2 infects iPSC-derived mature neurons

Based on the above findings in neurons of COVID-19 patients' brain cortexes, we propose that SARS-CoV-2 can effectively infect the CNS neurons. To establish an *in vitro* platform to study this process, we obtained iPSCs derived from age-matched healthy individuals and Alzheimer's patients and differentiated it into neurons, followed by SARS-CoV-2 infection. SARS-CoV-2-GFP (in which GFP replaced the viral open reading frame ORF7a [34]) at a multiplicity of infection (MOI) of 0.1 or 0.2 did not infect any cells at iPSC neuron differentiation day 35 (Fig. 5A, Supplementary Fig. 5A). Some of these cells expressed the pan-neuron marker Tuj1 but did not express the mature neuron marker NeuN (Fig. 5B, Supplementary Fig. 5B). At iPSC differentiation day 50, SARS-CoV-2-GFP at an MOI of 0.05, 0.1 or 0.2 effectively infected cells differentiated from iPSCs from healthy individuals and Alzheimer's patients (Fig. 5C, Supplementary Fig. 5C, D), and SARS-CoV-2-GFP could be detected in cell culture media 72 hours post SARS-CoV-2-GFP infection (Fig. 5D), indicating that the virus not only infects cells but also replicates intracellularly. SARS-CoV-2-infected cells were essentially all Tuj1-positive cells at iPSC differentiation day 50 (Fig. 5E), and no GFAP-positive astrocytes were detected in mock- and SARS-CoV-2-infected cells (Fig. 5F). At iPSC differentiation day 35, there was no expression of ACE2 or NRP1 proteins (Fig. 5G, H). At iPSC differentiation day 50, robust ACE2 and NRP1 protein expression existed in Tuj1-positive neurons (Fig. 5I, J). Over 40% of Tuj1-positive neurons were ACE2- and/or NRP1-positive (Fig. 5I, J). Subsequent experiments were conducted on iPSC differentiation day 50. These results suggest that SARS-CoV-2 infects mature neurons via ACE2 with the facilitation of NRP1.

SARS-CoV-2 induces Alzheimer's phenotypes in iPSC-derived cells

Because SARS-CoV-2 induces Aβ cellular aggregates and extracellular plaques, p-Tau cellular deposition and NFTs and neuroinflammation in COVID-19 patients, we hypothesized that SARS-CoV-2 infection can turn neurons derived from iPSCs of healthy individuals into AD-phenotype neurons. Neurons differentiated from iPSCs of healthy individuals and AD patients were infected with wild-type

SARS-CoV-2 (WA-1 strain [35]) at an MOI of 0.1 for 48 hours (Fig. 6). SARS-CoV-2 induced cellular Aβ aggregates in healthy neurons and increased cellular Aβ aggregates in Alzheimer's neurons (Fig. 6A). Cellular p-Tau deposition was induced in healthy neurons after 72 hours of SARS-CoV-2 infection (Fig. 6B), and the virus further increased cellular p-Tau deposition in Alzheimer's neurons (Fig. 6B). Compared to their mock-infected counterparts, both healthy neurons and Alzheimer's neurons had higher levels of major inflammatory cytokines including IL-1β, IL-6, IFNγ and TNFα after SARS-CoV-2 infection (Fig. 6C). Among the critical Alzheimer's mediators, amyloid precursor protein (APP), enzyme β-secretase 1 (BACE1), and presenilin 1/2 (PSEN1/2), SARS-CoV-2 significantly increased BACE1 expression in healthy neurons and Alzheimer's neurons but did not affect the expression of the other Alzheimer's mediators (Fig. 6D, E). Likewise, SARS-CoV-2 significantly increased the number of cleaved caspase 3-positive cells differentiated from iPSCs of healthy individuals and Alzheimer's patients (Fig. 6F). Thus, SARS-CoV-2 triggers an Alzheimer's-like cellular program in neurons derived from iPSCs of healthy individuals and enhances Alzheimer's phenotypes in cells derived from Alzheimer's iPSCs.

Alzheimer's infectious etiology genes identified via SARS-CoV-2

Over 95% of Alzheimer's cases are sporadic and their causes are still unclear. Studies of DNA viruses have shown that Alzheimer's etiology has an infectious component [36,37]. Based on the above observation that SARS-CoV-2 induces Alzheimer's phenotypes in neurons derived from iPSCs of healthy non-Alzheimer's individuals, we aimed to utilize SARS-CoV-2 infection to reveal genes responsible for the Alzheimer's infectious etiology. The transcriptomes of neurons differentiated from iPSCs of healthy individuals and Alzheimer's patients were determined by RNA sequencing (Fig. 7A-E). Under mock infection conditions, 553 genes were significantly upregulated, while 71 genes were significantly downregulated, in Alzheimer's neurons compared to neurons from iPSCs of healthy individuals (designated healthy neurons) (Fig. 7A). SARS-CoV-2 upregulated 75 genes and downregulated 19 genes

in healthy neurons (Fig. 7B). To extract the genes responsible for Alzheimer's infectious etiology, 24 overlapping genes were identified between the Alzheimer's neuron-mock-infected group and the healthy neuron-SARS-CoV-2-infected group (Fig. 7D). Pathway analysis revealed that the changes in these 24 genes activated infection pathways elicited by bacteria and viruses (Fig. 7D).

Compared to healthy neurons without viral infection, Alzheimer's neurons infected with SARS-CoV-2 had 517 upregulated genes and 256 downregulated genes (Fig. 7B). This number of downregulated genes (256) was higher than the number of downregulated genes in Alzheimer's neurons (71) (Fig. 7A, B). In Alzheimer's neurons, SARS-CoV-2 further increased the expression of 25 upregulated genes and decreased the expression of 34 downregulated genes by several-fold (Supplementary Fig. 6A, C), and pathway analysis pointed to the further activation of neuroinflammation and other processes in Alzheimer's neurons (Supplementary Fig. 6B, C).

Top upregulated genes in the Alzheimer's infectious etiology transform neurons

The 24 overlapping genes between Alzheimer's neurons without SARS-CoV-2 infection and healthy neurons infected by SARS-CoV-2 are potential genes involved in Alzheimer's infectious etiology. To evaluate whether the top upregulated genes among these 24 genes can turn healthy neurons into Alzheimer's-like neurons, we overexpressed the top three genes individually, FCGR3, LILRB5 and OTOR, in human primary neurons from a heathy individual. Overexpression of these genes in healthy neurons did not trigger cellular Aβ aggregation or cellular p-Tau deposition (Supplementary Fig. 6D). In contrast, when the top three downregulated genes in the 24-gene list, GJA8, CryAA2 and PSG6, were individually silenced in healthy human neurons, cellular expression of Aβ42 and p-Tau, cellular Aβ aggregation and cellular p-Tau deposition were induced (Fig. 7F, Supplementary Fig. 6E). Furthermore, silencing these top three downregulated genes simultaneously in healthy human neurons robustly triggered cellular Aβ aggregation and cellular p-Tau deposition (Fig. 7G). Thus, silencing the top three

downregulated genes reprogrammed healthy human neurons into Alzheimer's-like neurons.

Discussion

Although it is still controversial whether SARS-CoV-2 invades patients' brains [10,38], we provide strong evidence that SARS-CoV-2 can invade the cognitive centers of the brain, leading to AD-like neuro-phenotypes in both non-neurodegenerative disease and neurodegenerative disease individuals. Examination revealed that iPSC-derived neurons infected by SARS-CoV-2 recapitulated the key aspects related to clinically observed neurological disorders in COVID-19 patients and survivors: neurotropism and AD induction or enhancement of neurodegeneration by SARS-CoV-2.

Our observations from the brains of COVID-19 patients with underlying neurodegenerative disease or without such diseases support the effective infection of mature neurons by SARS-CoV-2. Thus, the present study demonstrates the neurotropism of SARS-CoV-2. Such neurotropism has long been known to occur for other types of human respiratory coronaviruses [39]. Consistent with the current findings, in human iPSC-derived brain sphere neurons, SARS-CoV-2 at a dose equivalent to that in the present study has been found to not only infect neurons but also replicate itself in these neurons [40]. The presence of the non-structural NSF2 protein indicates that SARS-CoV-2 may replicate in cortical neurons of infected brains. SARS-CoV-2 viral particles are present in both neuronal cell bodies and neurites [40]. SARS-CoV-2 can effectively infect cortical-like neurons in iPSC-derived brain organoids and these neurons express the SARS-CoV-2 receptor ACE2 and key coronavirus entry-associated proteases [41]. Regarding the infectibility of human brains by SARS-CoV-2, viral RNA has been detected in 36.4% of brain biopsies of fatal COVID-19 cases [9], suggesting that SARS-CoV-2 invades some COVID-19 patients' brains but may not invade all patients' brains. The current study examined cortical neurons of the brains of COVID-19 patients with or without neurodegenerative diseases and observed full infectibility by SARS-CoV-2 in all cases. Similarly, a recent study using spike protein staining demonstrated that SARS-CoV-2 was present in some brain regions in all three COVID-19 cases studied [10]. Using multiple approaches, we

showed the presence of spike and nucleocapsid proteins and SARS-CoV-2 viral particles in the cortical regions of all seventeen COVID-19 cases with or without neurodegenerative diseases.

An early study showed no evidence of SARS-CoV-2 infection of neurons [42]. In iPSC-derived brain organoids, SARS-CoV-2 infects only mature choroid plexus cells, not neurons or glial cells [42]. This discrepancy may be due to the different developmental stages of neurons. We show that iPSC-derived immature neurons do not express ACE2 and NPR1 and thus are not able to be infected by SARS-CoV-2, whereas mature neurons do express these two SARS-CoV-2 receptors and are infected by this virus. We also show that ACE2 is absent in neurons of the infant case, N and S protein are not detectable in this infant COVID-19 case, indicating that SARS-CoV-2 only infects or replicates in mature neurons *in vivo*. Pellegrini et al. [42] did not observe ACE2 expression in neurons. In COVID-19 patients, not all neurons are infected by SARS-CoV-2 [10], suggesting that different types of neurons have differential expression of ACE2 and other SARS-CoV-2 entry factors and variable SARS-CoV-2 infectability. Song et al. [10] have shown that cortical neurons including excitatory and inhibitory neurons, are able to be infected by SARS-CoV-2.

SARS-CoV-2 enters hosts through their noses, mouths, and eyes; thus, the anatomical proximity between the nasal cavity/nasopharynx and the olfactory mucosa may enable olfactory transmucosal entry of SARS-CoV-2 into the CNS [8]. The other major CNS entry route may depend on BBB leakage in conditions of autism and AD [12,13]. This may have been the case in our study, in which eight COVID-19 patients had either AD, other neurodegenerative diseases or autism. The BBB entry route is supported by a direct observation of BBB damage in COVID-19 patients [43]. Furthermore, the SARS-CoV-2 spike protein can disrupt human BBB integrity in 3D microfluidic *in-vitro* models [44]. Thus, SARS-CoV-2 may enter the CNS through multiple routes.

COVID-19 patients and survivors experience AD-like neural syndrome including memory loss,

delirium and cognitive deficits [25], suggesting that there is a cellular mechanism underlying these phenomena. A prior study showed altered distribution of tau from axons to soma and tau hyperphosphorylation in neurons of brain organoids exposed to SARS-CoV-2 [45]. We observed intracellular p-tau deposit in the cortexes of eleven adult COVID-19 cases without neurodegenerative diseases, suggesting that neurodegenerative characteristics manifest in COVID-19 patients' brains. Aβ deposition and neuroinflammation were also present in the cognitive centers of these COVID-19 patients and in iPSC-derived neurons infected by SARS-CoV-2. These observations potentially explain the AD-like brain disease observed in individuals exposed to SARS-CoV-2.

The pathogenesis of AD contains an element of infectious disease pathogenesis. Pathogen infections can lead to the onset and progression of AD. Insertions of viral DNA genomes into spontaneous late-onset AD patient genomes have been determined [36]. Viral DNA insertions in the host genome correlate with the induction of critical AD mediators, such as enzymes involved in Aβ species production, aggregation and plaque formation [36]. Direct evidence for the involvement of viral DNA in AD pathogenesis comes from the demonstration that herpes simplex virus type I (HSV-1) induces multicellular amyloid plaque–like structure formation, gliosis, and neuroinflammation in iPSC-derived neural cells and a 3D human brain-like model [37]. We provide direct evidence that the COVID-19 pandemic-causing virus SARS-CoV-2 triggers an AD-like molecular program involving a group of 24 genes related to infectious disease pathway activation. The β-secretase BACE1, which produces all monomeric forms of amyloid-β (Aβ), including Aβ42, was induced by SARS-CoV-2 in iPSC-derived neurons from healthy individuals; thus, BACE1 may be a primary driver of the AD-like phenotypes induced by SARS-CoV-2. SARS-CoV-2-induced hypoxia [10] may be responsible for BACE1 induction because hypoxia facilitates AD pathogenesis by inducing BACE1 expression [46]. Because 26 of the 29 SARS-CoV-2 proteins physically associate with many proteins in human cells [47], it is also possible that one or some of the 29 SARS-CoV-

2 proteins interact with transcriptional regulators in host cells, leading to BACE1 upregulation. The mechanism underlying SARS-CoV-2-induced AD-like phenotypes needs to be further investigated.

In summary, we found that SARS-CoV-2 infects the cortexes of COVID-19 patients with or without underlying neurodegenerative diseases. SARS-CoV-2 infection induced AD-like phenotypes in non-neurodegenerative disease patients and non-AD neurodegenerative disease patients, and exacerbated neuroinflammation in neurodegenerative disease patients. Neurodegenerative diseases enhance SARS-CoV-2 neuron infection. SARS-CoV-2 infection triggered cellular and molecular AD pathogenesis programs in iPSC-derived neurons from healthy individuals and enhanced neuropathological phenotypes in iPSC-derived neurons from AD patients. We reveal a list of 24 genes that potentially mediate the infectious etiology of AD under the condition of SARS-CoV-2 infection.

Methods

Brain Tissues

The major source for postmortem tissues is the NICHD neuro-tissue bank at the University of Maryland School of Medicine, and the Human Brain Collection Core, Intramural Research Program, National Institute of Mental Health (NIMH). The NICHD neuro-tissue bank is a national resource for investigators utilizing human post-mortem brain tissues and related biospecimens for research in understanding the conditions of the nervous system. All brain tissue is procured, stored, and distributed according to applicable State and Federal guidelines and regulations involving consent, protection of human subjects and donor anonymity. All brain tissues we obtained from the Brain Tissue Bank are de-identified. Formalin fixed brain tissues obtained from NIMH and neuro-tissue bank were further processed in sucrose solution and stored at 4°C.

Frozen brain tissues were also obtained from the Brain and Tissue Bank. The frozen tissues were used for RNA extraction followed by reverse transcription and PCR detection of SARS-CoV-2 with CDC specific primers. The frozen tissues include SARS-CoV-2 infected lung and brain tissues (6436), age-matched non-COV controls.

In addition, paraffin sections and frozen brain tissues of the subjects of COVID-19 FTD (1 case) and COVID-19 individual without underlying condition, and non-COV AD were obtained from the Biomarker Laboratory and Biorepository at University of Southern California Alzheimer's Therapeutic Research Institute (USC ATRI) at University of California San Diego (UCSD).

In situ hybridization/ RNAscope 2.5 HD Assay

RNAscope 2.5 HD Assay – RED was carried out to confirm the presence COVID-19 RNA in the brain samples following the ACD bio provided protocol. Simply, after peroxide treatment tissues were subjected for antigen retrieval. Antigen-retrieved and protease treated tissues were further incubated with specific

probe at 40°C. After successive amplification the presence of the antigen were detected with a Fast Red dye.

Immunohistochemistry and Immunofluorescence for brain sections

Immunohistochemistry was carried out as previously described [48,49]. Briefly, the coronal sections were rehydrated, and endogenous peroxidase was quenched by treating with 0.3% H_2O_2. For anti-Aβ (6E10) staining, the antigen retrieval was carried in 70% formic acid for 20 minutes. Antigen retrieval for the other antibodies was performed by autoclaving at 120°C for 10 min in citrate buffer. The primary antibody was applied on the sections at 4°C overnight, followed by 60-min incubation with specific secondary antibody coupled with HRP (Histofine simple stain MaxPo M/R, Nichirei Bioscience Inc., Japan) at room temperature. DAB (diaminobenzidine, 10mg/50ml, chromogen solution in PBS + 0.003% H_2O_2 (brown products) reaction was performed to visualize the color. For nucleocapsid and spike proteins, Ni-DAB were performed with DAB in 0.175 M sodium acetate + 0.5% nickel ammonium sulfate + 0.003% H_2O_2 (for Ni-DAB staining, black products) (*1)*. All antibody dilutions and washing steps were performed in phosphate buffer, pH 7.2. HRP intensities and cell counts in 3 different regions (example as Frontal Cortex, Entorhinal Cortex etc.) in three sections/slices from each group were measured using the ImageJ Fiji platform. Data were represented as number of positive cells/plaque/tangles per 100 μ m^2. Because the MaxPo M/R antibodies are Fab fragments, the blocking was not necessary.

DAB-stained sections were counterstained with hematoxylin. Sections were immersed in hematoxylin solution for 3 min and rinsed in running tap water until rinse water is colorless. Dehydrate and coverslip sequence: 70% ethanol, 3 minutes; 95% ethanol I and II, 3 minutes for each; 100% ethanol I and II, 3 minutes for each; xylene I and II, 5 minutes for each. Mounting medium: Permount Mounting Medium.

For immunofluorescence antigen retrieved brain sections were subjected for blocking with 10 % goat serum for 30 minutes followed by overnight incubation with specific primary antibody for overnight at

4°C. In the following day the brain sections were probed with Alexa-fluor labeled secondary antibody followed by nuclear staining with DAPI. Fluorescence was assessed using a fluorescence laser microscope (LSM780, Zeiss, Germany).

Thioflavin staining

The Aβ staining Thioflavin-T were performed following the similar antigen protocol. After blocking with 5% goat serum for 30 minutes, overnight incubation with anti Aβ antibody 6E10 were performed. In the following day the brain sections were probed with Alexa-fluor594 labeled secondary antibody. After an extensive washing, Thioflavin-T (0.1% in 50% DMSO) were applied over the brain sections for 5 minutes. An extensive washing was performed using PBS containing 0.05% tween20. Furthermore, the fluorescent background was quenched with Tureblack (Biotium, USA). Thioflavin-T and Alexa-fluor594 intensity were measured using a fluorescence laser microscope (LSM780, Zeiss, Germany).

Fluro Jade C Staining

Double staining with Fluro Jade C and anti-SARS-COV2 Nucleocapsid antibody were performed by following the protocol from the Fluro Jade C supplier (AG325, Merck) with some minor modifications. Brain sections obtaining from cryostat were mounted onto slides from and air-dried for 60 min on a slide warmer at 60°C followed by immersed in a basic alcohol solution consisting of 1% sodium hydroxide in 100% ethanol for 5 min, then 2 min in 70% ethanol and 2min in distilled water. The sections are then subjected to antigen retrieval by autoclaving at 120°C for 10 min in citrate buffer. After blocking with 5% goat serum and gelatin for 30 minutes, overnight incubation with anti-SARS-COV2 Nucleocapsid antibody were performed for overnight at 4°C. In the following day the brain sections were probed with Alexa-fluor594 labeled secondary antibody. An extensive washing was followed by 10 min in a solution

of 0.06% potassium permanganate. After washing with distilled water, the section were further stained for 10 min in a 0.0001% solution of FJ-C. The slides were then rinsed through ten changes of distilled water for 1min per change followed by DAPI. Excess water was drained onto a paper towel, and the slides were then air-dried. The air-dried slides were then cleared in xylene for 1 min and then cover slipped. Fluorescence intensities were measured using a fluorescence laser microscope (LSM780, Zeiss, Germany).

Generation of human induced pluripotent stem cells (hiPSCs)

Human fibroblast from Coriell Institute were induced into pluripotent stem cell with CMV promoter Thomson factors lentivirus set which contains Lenti-virus harboring Oct4, Sox2, Nanog, and Lin28 (Cat#: G353, ABM Inc., Canada). Briefly, human fibroblasts were seeded on 6 well plate with 8 x 10^4 per well at day -2 and transduced with Lenti-virus particles (MOI of 4:3:3:3). Cells were cultured for 7 days and replated at 2 x 10^4 cells per well of 6 well plate on irradiated mouse embryonic fibroblasts (MEF) feeder layer. From day 8, medium was replaced with Knockout DMEM (Invitrogen) supplemented with 20% Knockout Serum Replacer (KSR, Invitrogen), 0.1 mM nonessential amino acids (Invitrogen), 2 mM GlutaMAX (Invitrogen), 0.1 mM β-mercaptoethanol (Sigma-Aldrich, St. Louis, MO), 10 ng/ml recombinant human basic fibroblast growth factor (Invitrogen) (hiPSC medium). On week 3-4, iPSCs were identified from morphology change and picked out into 48-well plates with MEF feeder.

Mammalian iPSCs and culture conditions

Human iPSCs (4 cases of sporadic AD, and 6 cases of apparently healthy controls) purchased from the Coriell Institute for Medical Research were used in our study. iPSCs were maintained on irradiated mouse CF-1 feeder layer (ATCC, Manassas, VA) at 37 ºC and 5% CO_2 in Knockout DMEM medium (Invitrogen, Waltham, MA) supplemented with 20% Knockout Serum Replacer (KSR) (Invitrogen, Waltham, MA), 0.1 mM nonessential amino acids (Invitrogen, Waltham, MA), 2 mM GlutaMAX (Invitrogen, Waltham, MA), 0.1 mM β-Mercaptoethanol (Sigma-Aldrich, St. Louis, MO), 10 ng/ml recombinant human basic

fibroblast growth factor (Invitrogen, Waltham, MA) (hiPSC medium).

Neuron differentiation from hiPSCs.

hiPSCs were differentiated into neurons as described with modification[50]. hiPSCs dissociated with collagenase IV (Stem Cell Technologies) were cultured in suspension to form embryoid bodies (EB) in hES medium without bFGF for 5 days followed by maintenance in NIM medium containing Dulbecco's modified Eagle's medium/F12 and Neurobasal Medium (1:1, Thermo Fisher), 1% N2 Supplement (Life Technologies), 1% B27 Supplement (Life Technologies), nonessential amino acids, and 0.5% penicillin/streptomycin (Life Technologies) supplemented with inhibitors of the TGF-β receptor (SB431542, Stemgent; 5 μM) and the bone morphogenetic protein receptor (LDN-193189, Stemgent; 0.25 μM). On day 7, spheres were transferred to wells coated with Matrigel (BD Biosciences) and grown in NPM medium which is same to NIM medium but replace SB431542 and LDN-193189 with 10 ng/ml bFGF (PeproTech), 10 ng/mL epidermal growth factor (EGF) (PeproTech), and 2 μg/ml heparin (Sigma). On day 15, medium was changed to NDM medium which is same to NPM medium but replace bFGF, EGF and heparin in NPM with brain-derived neurotrophic factor (10 ng/ml; PeproTech), and glial cell–derived growth factor (10 ng/ml; PeproTech). Around day 20, neurons were observed and were further differentiated for 30 days.

Viral strains

Vero E6 cells were maintained in EMEM (ATCC) media with 10% Serum Plus II Medium Supplement (Sigma-Aldrich). SARS-CoV-2 virus were obtained from the CDC following isolation from a patient in Washington State (WA-1 strain - BEI #NR-52281). SARS-CoV-2 GFP was generously provided by Dr. Ralph S. Baric. Stocks were prepared by infection of Vero E6 cells.

SARS-CoV-2 production and infection of hiPSCs derived neurons

The stock of SARS-CoV-2 virus (CDC, WA-1 strain - BEI #NR-52281, and SARS-CoV-2 GFP generously

provided by Dr. Ralph S. Baric, at the Department of Epidemiology and Department of Microbiology and Immunology, the University of North Carolina at Chapel Hill, were prepared by infection of Vero E6 cells for two days when CPE (cytopathic effects) was starting to become visible. Media were collected and clarified by centrifugation prior to being aliquoted for storage at −80 °C. Neurons derived from hiPSCs were infected with SARS-CoV-2 at 1 x 10^4 per well of 6 well plate for 48 h in NDM medium. All work with the infectious virus was performed in a Biosafety Level 3 laboratory and approved by our Institutional Biosafety Committee.

Neural maturation, siRNA Transfection, and Lenti virus transduction

Primary Human Neurons obtained from Neuromics (Edina, MN) grow for four weeks in the Neuromics growth medium supplemented with brain derived neurotropic factor (BDNF). Medium were changed every 2 days. For further experiment, cells were plated on a 6-well plate in neuron growth medium supplemented with 5% FBS, BDNF and 1.0 μM qretinoic acid (Merck / MilliporeSigma, USA). siRNA transfection was carried out using X-tremeGENE siRNA transfection reagent (Roche, Basel, Switzerland) at 60% cell confluency. Medium was replaced with fresh medium 24 hours post-transfection and maintained for additional 48 hours. Lentivirus mediated overexpression of the FCGR, LILRB5 and OTOR carried out using virus particles obtained from OriGene (Rockville, MD). Virus transduction were carried out at 5.0 MOI using polybrene. GFP expressing lenti-particles were used as the control.

RNA sequencing

mRNAs were extracted from neurons derived from AD or Control hiPSCs with or without SARS-CoV-2 infection and sequenced at BGI on DNBSeq platform. Briefly, mRNAs were extracted with Trizol reagent. First-strand cDNA was generated using random hexamer-primed reverse transcription, followed by a second-strand cDNA synthesis. The synthesized cDNA was subjected to end-repair and then was 3' adenylated. Adapters were ligated to the ends of these 3' adenylated cDNA fragments, followed by PCR.

PCR products were purified with Ampure XP Beads and dissolved in EB solution. The library was validated on the Agilent Technologies 2100 bioanalyzer. The double stranded PCR products were heat denatured and circularized by the splint oligo sequence. The single strand circle DNA was formatted as the final library. The library was amplified with phi29 to make DNA nanoball (DNB) which had more than 300 copies of one molecular. The DNBs were loaded into the patterned nanoarray and single end 50 (pair end 100) bases reads were generated in the way of sequencing by synthesis.

Immunofluorescent staining for neuronal Cells

For immunofluorescence staining, cells were cultured on a collagen-coated coverslip. After specific treatments, cells were fixed with 4% paraformaldehyde-PBS. The cell membrane was permeabilized with 0.25% Triton-X100 and/or 5 mg/ml digitonin followed by blocking with 5% BSA. After probing with primary antibodies, specific Alexa-fluor labeled secondary antibody were used. 4',6-Diamidino-2-phenylindole dihydrochloride (DAPI) staining was used to visualize the nuclei (Thermo Fisher Scientific). Fluorescence was assessed using a fluorescence laser microscope (LSM780, Zeiss, Germany).

Quantitative reverse transcription PCR

mRNAs were extracted from neurons derived from AD or Control hiPSCs with or without SARS-CoV-2 infection in Trizol reagent (Thermofisher, Waltham, MA) and followed by cDNA synthesis with SuperScript™ III Reverse Transcriptase kit (ThermoFisher). RT-PCR were performed with PowerUp™ SYBR™ Green Master Mix (ThermoFisher) with 45 cycles and PCR products were loaded into 2% agarose gel and run at 75 v for 5.5 h. Gel Image were recorded with Bio-Rad ChemiDoc MP imaging system (Hercules, CA).

Quantification and Statistical analysis

In the experiment assessing the impact of SARS-CoV-2 virus on the brain pathology, we analyzed (a) 17 COVID19 samples, 17 cases of age-matched controls. Labeled cells from at least 3 random fields ($n \geq 3$)

were counted and expressed as number of cells per 100 μm^2. Data are presented as the means ± standard errors (SEs). All statistical analysis was performed using JMP 13.0 software. Student's t test and Mann-Whitney U test were used for two group comparisons based on data distribution. Two-way ANOVA was performed for comparisons of more than two group. In ANOVA, a *Tukey* test was used to estimate the significance between groups.

In the experiment with cell culture studies, we differentiated neurons from 6 iPSC lines derived from AD fibroblast cells and 6 lines from healthy subjects as the controls. The experiments were repeated in triplicate as we previously described [51,52]. Data are presented as the means ± standard errors (SEs).

Acknowledgments

This work was supported by NIH grants R01HD100195, R01HD102206, R01HD099843, R01DK083243, R01DK101972, R01HL131737, R01HL134368, R01HL139060, R01DK103024 and P30-AG062429. No potential conflicts of interest relevant to this article are reported. Human brain tissue was obtained from the NIMH Human Brain Collection Core. The authors thank Jeffrey Metcalf, Sara Shuldberg and Sophia Perrott from the Rissman lab and UCSD Shiley-Marcos ADRC for technical assistance with this project.

Author Contributions

Shen WB, Montasir E, Penghua Yang, Xu C, Logue J, and Baracco L researched and analyzed the data. Frieman M, Reece EA, Blanchard T, Li L, Han Z, and Rissman R analyzed the data and revised the manuscript. Peixin Yang conceived the project and wrote the manuscript. All authors approved the final version of the paper.

Declaration of Interests

The authors declare no competing interests.

References

1. Helms, J., *et al.* Neurologic Features in Severe SARS-CoV-2 Infection. *N Engl J Med* **382**, 2268-2270 (2020).
2. Mao, L., *et al.* Neurologic Manifestations of Hospitalized Patients With Coronavirus Disease 2019 in Wuhan, China. *JAMA Neurol* **77**, 683-690 (2020).
3. de Erausquin, G.A., *et al.* The chronic neuropsychiatric sequelae of COVID-19: The need for a prospective study of viral impact on brain functioning. *Alzheimers Dement* (2021).
4. Taquet, M., Geddes, J.R., Husain, M., Luciano, S. & Harrison, P.J. 6-month neurological and psychiatric outcomes in 236 379 survivors of COVID-19: a retrospective cohort study using electronic health records. *Lancet Psychiatry* **8**, 416-427 (2021).
5. De Santis, G. SARS-CoV-2: A new virus but a familiar inflammation brain pattern. *Brain Behav Immun* **87**, 95-96 (2020).
6. Li, K., *et al.* Middle East Respiratory Syndrome Coronavirus Causes Multiple Organ Damage and Lethal Disease in Mice Transgenic for Human Dipeptidyl Peptidase 4. *J Infect Dis* **213**, 712-722 (2016).
7. Netland, J., Meyerholz, D.K., Moore, S., Cassell, M. & Perlman, S. Severe acute respiratory syndrome coronavirus infection causes neuronal death in the absence of encephalitis in mice transgenic for human ACE2. *J Virol* **82**, 7264-7275 (2008).
8. Meinhardt, J., *et al.* Olfactory transmucosal SARS-CoV-2 invasion as a port of central nervous system entry in individuals with COVID-19. *Nat Neurosci* **24**, 168-175 (2021).
9. Puelles, V.G., *et al.* Multiorgan and Renal Tropism of SARS-CoV-2. *N Engl J Med* **383**, 590-592 (2020).
10. Song, E., *et al.* Neuroinvasion of SARS-CoV-2 in human and mouse brain. *J Exp Med* **218**(2021).
11. Zheng, J., *et al.* COVID-19 treatments and pathogenesis including anosmia in K18-hACE2 mice. *Nature* **589**, 603-607 (2021).
12. Montagne, A., Zhao, Z. & Zlokovic, B.V. Alzheimer's disease: A matter of blood-brain barrier dysfunction? *J Exp Med* **214**, 3151-3169 (2017).
13. Fiorentino, M., *et al.* Blood-brain barrier and intestinal epithelial barrier alterations in autism spectrum disorders. *Mol Autism* **7**, 49 (2016).
14. Iadecola, C., Anrather, J. & Kamel, H. Effects of COVID-19 on the Nervous System. *Cell* **183**, 16-27 e11 (2020).
15. Hoffmann, M., *et al.* SARS-CoV-2 Cell Entry Depends on ACE2 and TMPRSS2 and Is Blocked by a Clinically Proven Protease Inhibitor. *Cell* **181**, 271-280 e278 (2020).
16. Butowt, R. & Bilinska, K. SARS-CoV-2: Olfaction, Brain Infection, and the Urgent Need for Clinical Samples Allowing Earlier Virus Detection. *ACS Chem Neurosci* **11**, 1200-1203 (2020).
17. Cantuti-Castelvetri, L., *et al.* Neuropilin-1 facilitates SARS-CoV-2 cell entry and infectivity. *Science* **370**, 856-860 (2020).
18. Vanacker, C., *et al.* Neuropilin-1 expression in GnRH neurons regulates prepubertal weight gain and sexual attraction. *EMBO J* **39**, e104633 (2020).
19. Rogers, J.P., *et al.* Psychiatric and neuropsychiatric presentations associated with severe coronavirus infections: a systematic review and meta-analysis with comparison to the COVID-19 pandemic. *Lancet Psychiatry* **7**, 611-627 (2020).
20. Varatharaj, A., *et al.* Neurological and neuropsychiatric complications of COVID-19 in 153 patients: a UK-wide surveillance study. *Lancet Psychiatry* **7**, 875-882 (2020).
21. Paterson, R.W., *et al.* The emerging spectrum of COVID-19 neurology: clinical, radiological and laboratory findings. *Brain* **143**, 3104-3120 (2020).
22. Kadono, Y., *et al.* A case of COVID-19 infection presenting with a seizure following severe brain edema. *Seizure* **80**, 53-55 (2020).
23. Hosseini, A.A., Shetty, A.K., Sprigg, N., Auer, D.P. & Constantinescu, C.S. Delirium as a presenting feature in COVID-19: Neuroinvasive infection or autoimmune encephalopathy? *Brain Behav Immun* **88**, 68-70 (2020).

24. Alkeridy, W.A., *et al.* A Unique Presentation of Delirium in a Patient with Otherwise Asymptomatic COVID-19. *J Am Geriatr Soc* **68**, 1382-1384 (2020).
25. Jaywant, A., *et al.* Frequency and profile of objective cognitive deficits in hospitalized patients recovering from COVID-19. *Neuropsychopharmacology* (2021).
26. Heneka, M.T., Golenbock, D., Latz, E., Morgan, D. & Brown, R. Immediate and long-term consequences of COVID-19 infections for the development of neurological disease. *Alzheimers Res Ther* **12**, 69 (2020).
27. Vallamkondu, J., *et al.* SARS-CoV-2 pathophysiology and assessment of coronaviruses in CNS diseases with a focus on therapeutic targets. *Biochim Biophys Acta Mol Basis Dis* **1866**, 165889 (2020).
28. Wang, Q., Davis, P.B., Gurney, M.E. & Xu, R. COVID-19 and dementia: Analyses of risk, disparity, and outcomes from electronic health records in the US. *Alzheimers Dement* (2021).
29. Coil, D.A., *et al.* SARS-CoV-2 detection and genomic sequencing from hospital surface samples collected at UC Davis. *PLoS One* **16**, e0253578 (2021).
30. Schmued, L.C., Stowers, C.C., Scallet, A.C. & Xu, L. Fluoro-Jade C results in ultra high resolution and contrast labeling of degenerating neurons. *Brain Res* **1035**, 24-31 (2005).
31. Ehara, A. & Ueda, S. Application of Fluoro-Jade C in acute and chronic neurodegeneration models: utilities and staining differences. *Acta Histochem Cytochem* **42**, 171-179 (2009).
32. Gomez-Isla, T., *et al.* Neuronal loss correlates with but exceeds neurofibrillary tangles in Alzheimer's disease. *Ann Neurol* **41**, 17-24 (1997).
33. Giannakopoulos, P., *et al.* Tangle and neuron numbers, but not amyloid load, predict cognitive status in Alzheimer's disease. *Neurology* **60**, 1495-1500 (2003).
34. Hou, Y.J., *et al.* SARS-CoV-2 Reverse Genetics Reveals a Variable Infection Gradient in the Respiratory Tract. *Cell* **182**, 429-446 e414 (2020).
35. Tian, J.H., *et al.* SARS-CoV-2 spike glycoprotein vaccine candidate NVX-CoV2373 immunogenicity in baboons and protection in mice. *Nat Commun* **12**, 372 (2021).
36. Readhead, B., *et al.* Multiscale Analysis of Independent Alzheimer's Cohorts Finds Disruption of Molecular, Genetic, and Clinical Networks by Human Herpesvirus. *Neuron* **99**, 64-82 e67 (2018).
37. Cairns, D.M., *et al.* A 3D human brain-like tissue model of herpes-induced Alzheimer's disease. *Sci Adv* **6**, eaay8828 (2020).
38. Thakur, K.T., *et al.* COVID-19 neuropathology at Columbia University Irving Medical Center/New York Presbyterian Hospital. *Brain* (2021).
39. Arbour, N., Day, R., Newcombe, J. & Talbot, P.J. Neuroinvasion by human respiratory coronaviruses. *J Virol* **74**, 8913-8921 (2000).
40. Bullen, C.K., *et al.* Infectability of human BrainSphere neurons suggests neurotropism of SARS-CoV-2. *ALTEX* **37**, 665-671 (2020).
41. Zhang, B.Z., *et al.* SARS-CoV-2 infects human neural progenitor cells and brain organoids. *Cell Res* **30**, 928-931 (2020).
42. Pellegrini, L., *et al.* SARS-CoV-2 Infects the Brain Choroid Plexus and Disrupts the Blood-CSF Barrier in Human Brain Organoids. *Cell Stem Cell* **27**, 951-961 e955 (2020).
43. Alexopoulos, H., *et al.* Anti-SARS-CoV-2 antibodies in the CSF, blood-brain barrier dysfunction, and neurological outcome: Studies in 8 stuporous and comatose patients. *Neurol Neuroimmunol Neuroinflamm* **7**(2020).
44. Buzhdygan, T.P., *et al.* The SARS-CoV-2 spike protein alters barrier function in 2D static and 3D microfluidic in-vitro models of the human blood-brain barrier. *Neurobiol Dis* **146**, 105131 (2020).
45. Ramani, A., *et al.* SARS-CoV-2 targets neurons of 3D human brain organoids. *EMBO J* **39**, e106230 (2020).
46. Sun, X., *et al.* Hypoxia facilitates Alzheimer's disease pathogenesis by up-regulating BACE1 gene expression. *Proc Natl Acad Sci U S A* **103**, 18727-18732 (2006).
47. Gordon, D.E., *et al.* A SARS-CoV-2 protein interaction map reveals targets for drug repurposing. *Nature* **583**, 459-

468 (2020).

48. Elahi, M., *et al.* Region-Specific Vulnerability to Oxidative Stress, Neuroinflammation, and Tau Hyperphosphorylation in Experimental Diabetes Mellitus Mice. *J Alzheimers Dis* **51**, 1209-1224 (2016).
49. Elahi, M., *et al.* High-fat diet-induced activation of SGK1 promotes Alzheimer's disease-associated tau pathology. *Hum Mol Genet* **30**, 1693-1710 (2021).
50. Wang, C., *et al.* Gain of toxic apolipoprotein E4 effects in human iPSC-derived neurons is ameliorated by a small-molecule structure corrector. *Nat Med* **24**, 647-657 (2018).
51. Cheng, X., *et al.* Maternal diabetes induces senescence and neural tube defects sensitive to the senomorphic rapamycin. *Science Advances* **7**, eabf5089 (2021).
52. Wang, F., *et al.* Ask1 gene deletion blocks maternal diabetes-induced endoplasmic reticulum stress in the developing embryo by disrupting the unfolded protein response signalosome. *Diabetes* **64**, 973-988 (2015).

Figure legend

Fig. 1. SARS-CoV-2 is present in cortical cells of COVID-19 patients.

(A) Representative images of SARS-CoV-2 RNA *in situ* hybridization in the entorhinal cortexes of COVID-19 and non-COVID-19 human brains. 12 cases of COVID-19 with no underlying neurodegenerative diseases (NND) are presented in the upper two panels. The third panel represents the non-COVID-19 controls without or with underlying neurodegenerative diseases (ND) (Supplementary Table 1). The lowest (fourth) panel represents five COVID-19 cases with different ND (AD, FTD, Dementia, LBD, and PSP). The brain IDs are presented at the top left. Higher magnification images are presented in the inset. SARS-CoV-2 RNA signal is pointed by arrows. Scale bar 25 µm. **(B)** A statistical comparison of the SARS-CoV-2 RNA (red dot per 100 μm^2) in two different groups (NND and ND) is presented in the bar graph. For each case, 3 independent images from three different fields were included for analysis. Data were analyzed by the Mann-Whitney U test after confirming the data distribution. Distribution of the SARS-CoV-2 RNA in 3 different regions of the brain including the entorhinal cortex (Ent), Inferior-Prefrontal cortex (IPC), and dorsolateral Prefrontal Cortex (DPC), was shown. +++ indicates 20-30- virus particles per 100 μm^2, ++ indicates 10-20 virus particles per 100 μm^2, and + indicates 1-10- virus particles per 100 μm^2. (**C**) Representative images of SARS-CoV-2 nucleocapsid protein (NC) in the Ent of COVID-19 and non-COVID-19 cases. Infected brains without underlying ND are presented in the upper two panels. The third panel represents the non-COVID-19 control. The fourth panel represents the COVID-19 cases with different ND. Nucleocapsid protein signals were visualized with a DAB-Nickel, in a reaction of horse radish peroxidase (HRP)-coupled with anti-rabbit secondary antibody (Fab fragments). SARS-CoV-2 NC protein black dot signals were located in the cytosol of the neuronal cells (indicated by red arrows). The brain IDs are presented at the top left. Scale bar 25 µm. (D) A statistical comparison of the nucleocapsid (NC) positive cells in the Ent for NND (non-

neurodegenerative disease) and ND cases are presented in the bar graph. For each case, 3 independent images from three different fields were included for analysis. Data were analyzed by the Mann-Whitney U test after confirming the data distribution. Quantification of the NC positive cells in 3 different regions of the brain including Ent, IPC, and DPC. +++ indicates 2-3 capsid protein positive cells per 100 μm^2, ++ indicates 1-2 capsid protein positive cells per 100 μm^2, and + indicates 0-1 capsid protein positive cells per 100 μm^2.

Fig. 2. hACE2-positive positive neurons exhibit SARS-CoV-2 positivity and undergo neurodegeneration.

(**A**) Immunofluorescence observation of MAP2 (Red) and hACE2 (Green)-positive cells in the Ent of the COVID-19 adult brain (indicated) (Case #3170), and the COVID-19 infected infant (3177) brain. Scale bar 50 µm. (**B**) Comparison of the hACE2 expression in the brain microvasculature and the neuronal cells present in the adult brain 3170. The cytoplasmic expression of the hACE2 is presented in a neuron (indicated) enlarged in the inset. Scale bar 50 µm. (**C**) hACE2 was colocalized with Capsid in immunofluorescence observation of Capsid (Red) and hACE2 (Green)-positive neuronal cells in the Ent of the COVID-19 adult brain. Scale bar 5 µm. (**D**) *In situ* hybridization of SARS-CoV-2 RNA with immunochemical staining with anti-NeuN showed the presence of the viral RNA in neurons. Scale 5 µm. (**E**) Immunofluorescence analysis of Capsid (Red) and NeuN (Green)-positive cells in the Ent of the SARS-CoV-2 infected adult brain (6609) but not in the non-COVID-19 control (6381). Scale bar 50 µm. (**F**) Immunohistochemical analysis of the SARS-CoV-2 non-structural protein NSP2 in COVID-19 adult patients' brain (6609, 3170), infant (3177). Scale bar 50 µM. (**G**) Capsid protein-positive neurons undergo neurodegeneration. Immunofluorescence analysis of Capsid (Red signals) and Fluro-Jade C (Green signals)-positive cells in the Ent of the SARS-CoV-2 infected brain (3170) and non-COVID-19 controls. A lower magnification image is presented (scale bar 100 µm) and a higher magnification (inset) showing

the presence of the NC protein in degenerating neuron. The degenerating neurons in 4 different groups are counted (3 images for each case) and analyzed by two-way ANOVA followed by Tukey HSD and *P*-values indicated in the graphs.

Fig. 3. SARS-CoV-2 infection induces or enhances cellular Aβ aggregation and Tau phosphorylation

(**A**) Aβ immunohistochemical staining (with the anti-Aβ antibody 6E10) in the Ent region of SARS-CoV-2 infected non-neurodegenerative cases (total 12; upper two panels), non-COVID-19 controls (third panel) and SARS-CoV-2 infected neurodegenerative cases (5 different types of neurodegenerative cases; fourth panel). Intracellular/cytoplasmic deposition of Aβ (red arrow) and extracellular amyloid plaque (yellow arrow) are indicated. Scale bar 25 μm for NND and 50 μm for ND. (**B**) Immunofluorescence analysis with thioflavin-T (green signal) and Aβ (red signal) indicated that the cytoplasmic deposits of Aβ in the SARS-CoV-2 infected non-neurodegenerative cases consisted of aggregated Aβ. Scale bar 50 μm (**C**) Quantification of cellular Aβ deposits in non-neurodegenerative cases per 100 μm^2 (3 independent images for one case). Data were analyzed by Mann-Whitney U test after confirming the data distribution. Distribution of the intracellular/cytoplasmic deposition of Aβ in SARS-CoV-2 infected non-neurodegenerative cases (NND) and extracellular amyloid plaque in SARS-CoV-2 infected neurodegenerative cases in 3 different regions of the brains including the entorhinal cortex (Ent), Inferior-Prefrontal cortex (IPC) and dorsolateral Prefrontal Cortex (DPC) (left). +++ indicates 2-3 Aβ-positive cells per 100 μm^2, ++ indicates 1-2 Aβ-positive cells per 100 μm^2, and + indicates 0-1 Aβ-positive cells per 100 μm^2. (**D**) p-Tau (pSer202) immunostaining in the Ent region of SARS-CoV-2 infected non-neurodegenerative cases (total 12; upper two panels), non-COVID-19 controls (third panel) and SARS-CoV-2 infected neurodegenerative cases (5 different types of neurodegenerative cases; fourth panel). Intracellular/cytoplasmic deposition of p-Tau (red arrow) and aggregated tau deposit (tangles, astrocytic

tau deposit, etc.; yellow arrow) are indicated. Scale bar 25 μm. (**E**) Immunofluorescence analysis of p-Tau (pSer202; green signal) and SARS-CoV-2 Capsid (red signal) showed Covid infected cells represent tau hyperphosphorylation. Scale bar 25 μm (**F**) Quantification of cellular p-Tau deposition per 100 μm^2 (3 independent images for one case). Significant *P*-values are indicated (by Mann-Whitney U test after confirming the data distribution). +++ indicates 2-3 pTau-positive cells per 100 μm^2, ++ indicates 1-2 pTau -positive cells per 100 μm^2, and + indicates 0-1 pTau -positive cells per 100 μm^2.

Fig. 4. Neuroinflammation in the cortical regions of SARS-CoV-2 infected brain.

(**A**) Representative images of microglial immunohistochemical staining (with the anti-ibaI antibody) in the Ent region of SARS-CoV-2 infected non-neurodegenerative cases (total 12; upper two panels), non-COVID-19 controls (third panel) and SARS-CoV-2 infected neurodegenerative cases (5 different types of neurodegenerative cases; fourth panel). Activated microglia (red arrow) are indicated. Scale bar 25 μM. (**C**) Interleukin-6 (IL-6) immunohistochemical staining in the Ent region of SARS-CoV-2 infected non-neurodegenerative cases (total 12; upper two panels), non-COVID-19 controls (third panel) and SARS-CoV-2 infected neurodegenerative cases (5 different types of neurodegenerative cases; fourth panel). IL-6 positive neurons (red arrow) are indicated. Scale bar 50 μM. The graphs show the number of activated microglia (**B**) and IL-6 positive neurons **(D)** per 100 μm^2 (3 independent images for one section). Graphs are represented as the means ± SEM and were analyzed by two-way ANOVA followed by Tukey HSD and *P*-values indicated in the graphs. +++ indicates 8-12 activated microglial cells per 100 μm^2, ++ indicates 4-8 activated microglial cells per 100 μm^2, and + indicates 0-4 activated microglial cells per 100 μm^2.

Fig. 5. SARS-CoV-2 infects mature neurons derived from human iPSCs.

(**A**). SARS-CoV-2-GFP does not infect immature neurons at iPSC neuron differentiation day 35 (n = 3 replicates). (**B**). Immature neurons do not express the mature neuron marker, NeuN. (**C**). SARS-CoV-2

infects mature neurons at iPSC neuron differentiation day 50 (n = 3). (**D**). Detection of SARS-CoV-2 in the culture medium of infected neurons (n = 3). (**E**). SARS-CoV-2 infects Tuj1-positive neurons (n = 3). (**F**). GFAP is not expressed in SARS-CoV-2-infected cells at iPSC differentiation day 50 (n = 2). Immature Tuj1-positive neurons do not express ACE2 (**G**) and NRP1 (**H**) (n = 3). Mature Tuj1 positive neurons express ACE2 (**I**) and NRP1 (**J**) (n = 3). The bars show the percentages of double Tuj1- and ACE2- or NRP1-positive cells (yellow) among total $Tuj1^{+}$ cells (green) (n = 3). AD: Alzheimer's disease; CTL: control group (non-AD); ACE2: angiotensin-converting enzyme 2; Tuj1: beta-Tubulin III; NRP1: Neuropilin 1; SPIKE: SARS-CoV-2 spike protein.

Fig. 6. SARS-CoV-2 induces or enhances Alzheimer's-like neuron phenotypes.

(**A**). SARS-CoV-2 induces cellular Aβ aggregation in neurons derived from iPSCs of healthy individuals and Alzheimer's patients (n = 3 iPSC lines). (**B**). SARS-CoV-2 induces cellular p-Tau deposition in neurons derived from iPSCs of healthy individuals and Alzheimer's patients (n = 3 iPSC lines). The values in the graphs are presented as the means ± SEMs (n = 5 images from 2 independent experiments for each group). The Aβ and p-Tau intensity data were analyzed by Mann-Whitney U test after confirming a normal distribution. Bars = 50 μm. mRNAs levels of inflammatory cytokines (**C**), BACE1 (**D**), and Alzheimer's molecular mediators (APP, PSEN1 and PSEN2) (**E**) in SARS-CoV-2-infected neurons derived from iPSCs (n = 6, 3 iPSC lines for 2 independent experiments). **(F).** Cleaved caspase 3 (c-Cas3)-positive cells in SARS-CoV-2 infected neurons derived from iPSCs (n = 6 iPSC lines for 2 independent experiments). The bar graph shows the quantification of c-Cas3-positive cell numbers. CTL: control group (iPSCs from healthy individuals); AD: Alzheimer's disease; CTLv: SARS-CoV-2-infected control group; ADv: SARS-CoV-2-infected AD group; Tuj1: beta-Tubulin III; c-Cas3, cleaved caspase 3. Data were analyzed by Mann-Whitney U test after confirming a normal distribution, significant *P*-values are presented.

Fig. 7. Identification of an infectious etiology gene signature for Alzheimer's disease.

(**A**). Volcano plot of differentially expressed genes (DEGs) in neurons derived from iPSCs of patients with Alzheimer's disease (AD) (the AD group) compared to neurons derived from iPSCs of healthy individuals (the CTL group). (**B**). Volcano plot of DEGs in healthy individual iPSC-derived neurons infected with SARS-CoV-2 (the CTL_V group) compared to the CTL group. (**C**). Volcano plot of DEGs in AD neurons infected with SARS-CoV-2 (the AD_V group) compared to the CTL group. (**D**). Venn plot and KEGG pathway analysis for DEGs between the AD group and the CTL_V group. The CTL group served as the baseline group. The twenty-four overlapping genes constituted the AD infectious etiology gene signature. (**E**). Venn plot and KEGG pathway analysis for DEGs between the AD group and the AD_V group. The CTL group served as the baseline group. For **A** to **E**, n = 3 iPSC lines for the CTL and AD groups. (**F-G**). Analysis of the effect of siRNA mediated individual or combined knockdown of the top 3 downregulated genes, GJA8, CryAA2 and PSG6, on the AD infectious etiology gene signature in primary human neurons. **F**: Immunoblot analysis of Aβ isoforms in siRNA transfected cells (n = 3 replicates). **G**. Cellular Aβ aggregation (left panel) and cellular p-Tau deposition (right panel). Aβ aggregates and p-Tau accumulation in the cytoplasm or neuronal axon are indicated by white arrowheads. The values in the graphs are presented as the means ± SEMs (n = 8 images from 3 replicates). Intensity data were analyzed by Mann-Whitney U test after confirming a normal distribution, significant *P*-values are presented. Scale bar, 50 μm.

Fig. 1

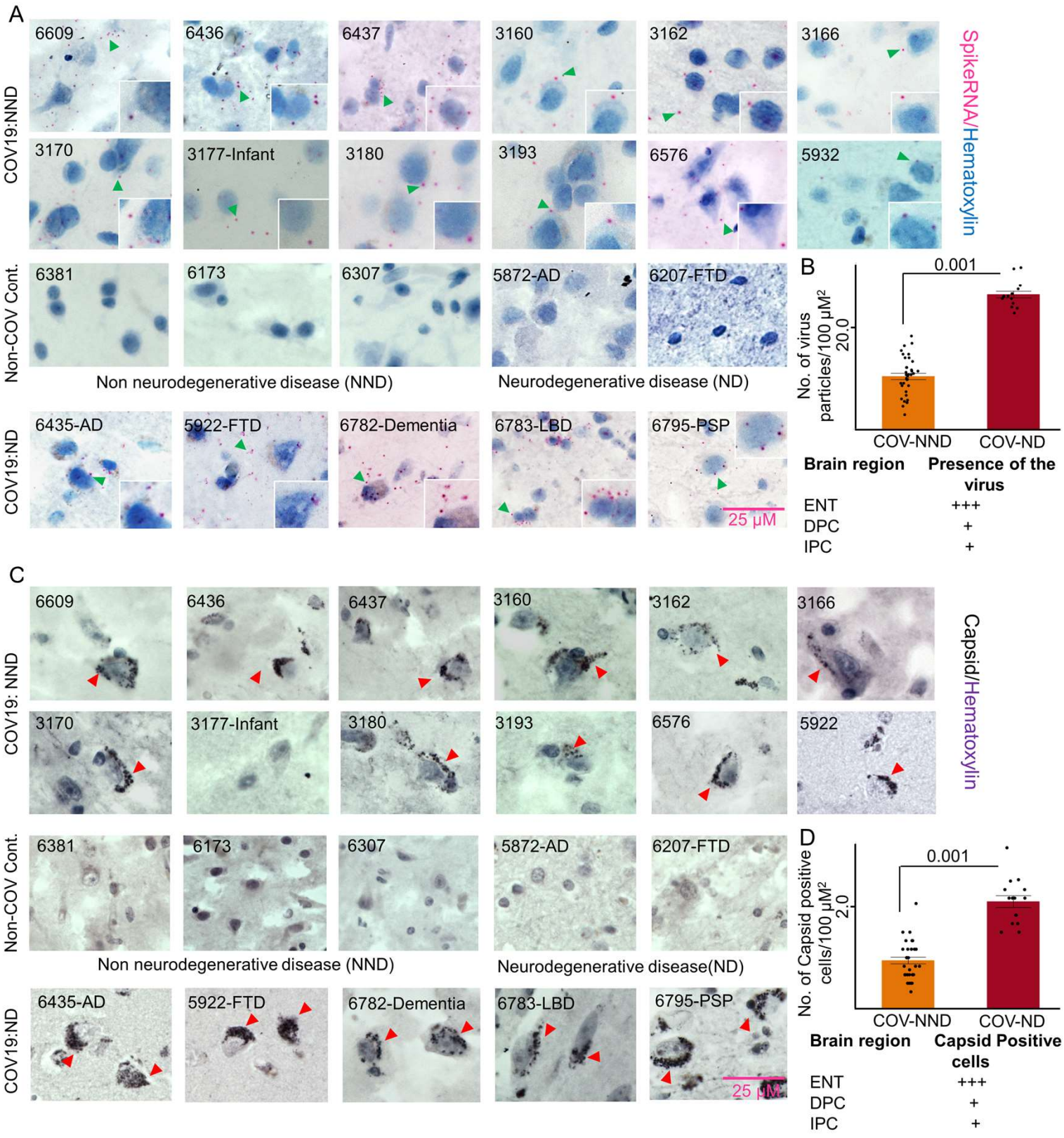

Fig. 2

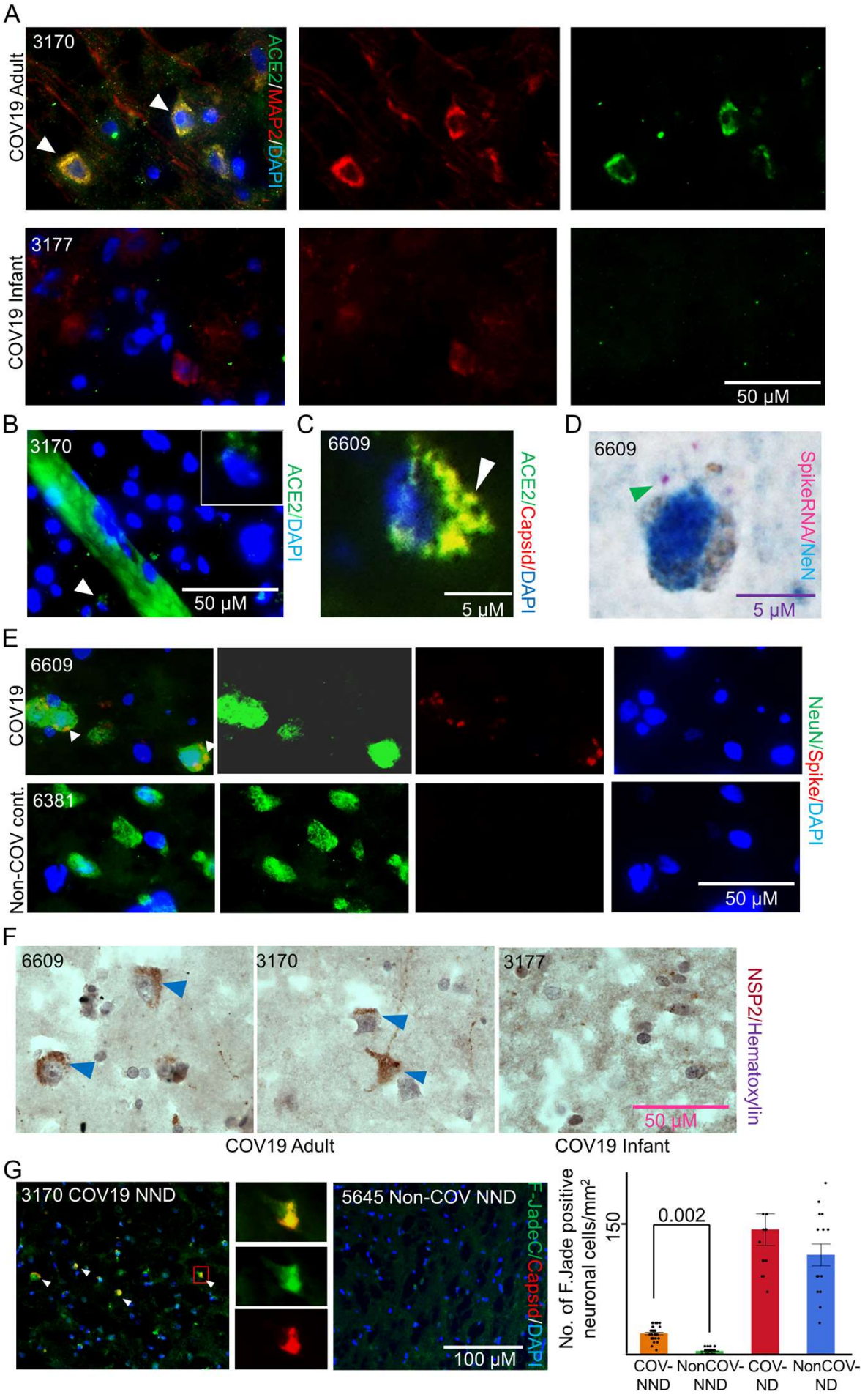

Fig. 3

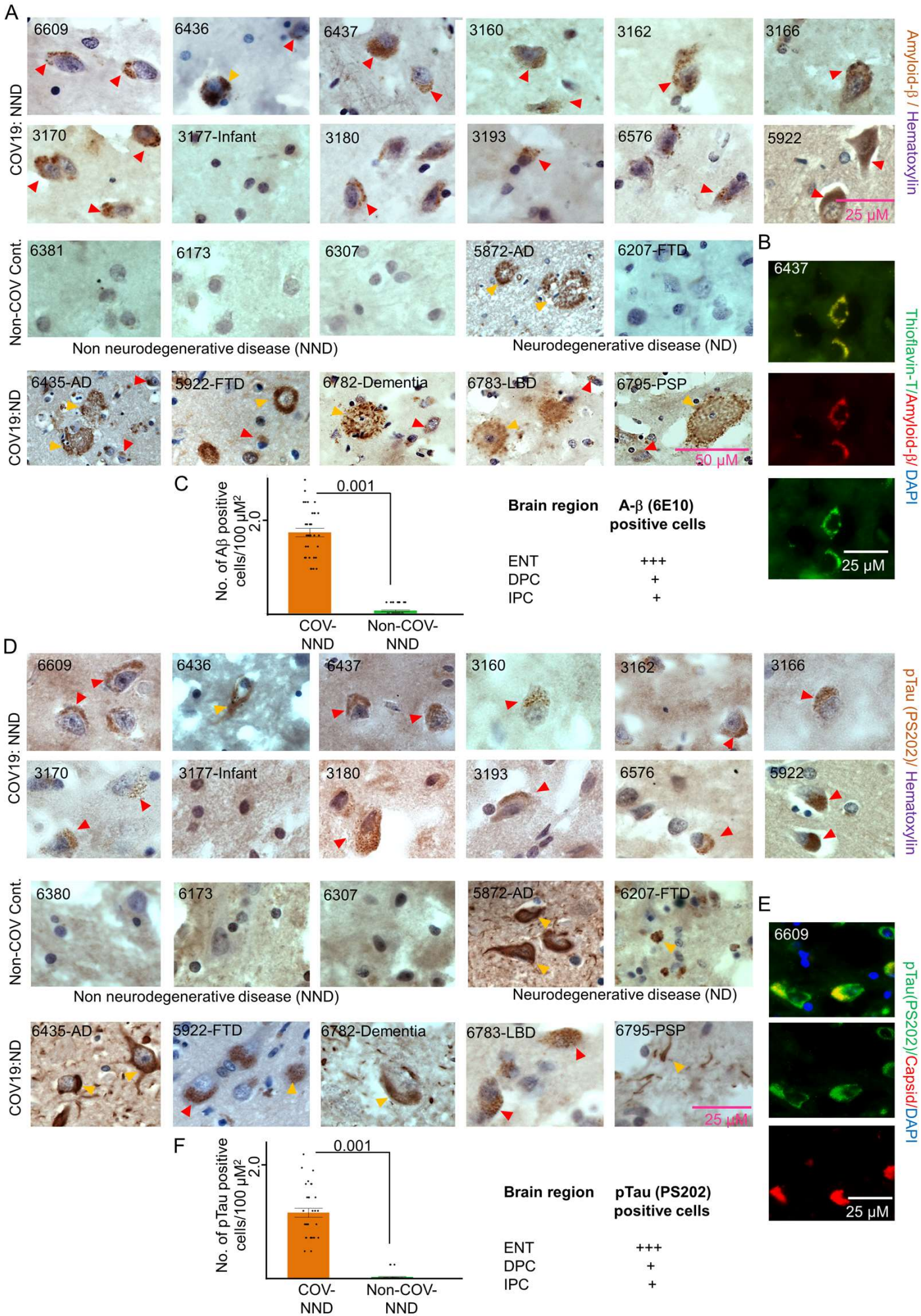

Fig. 4

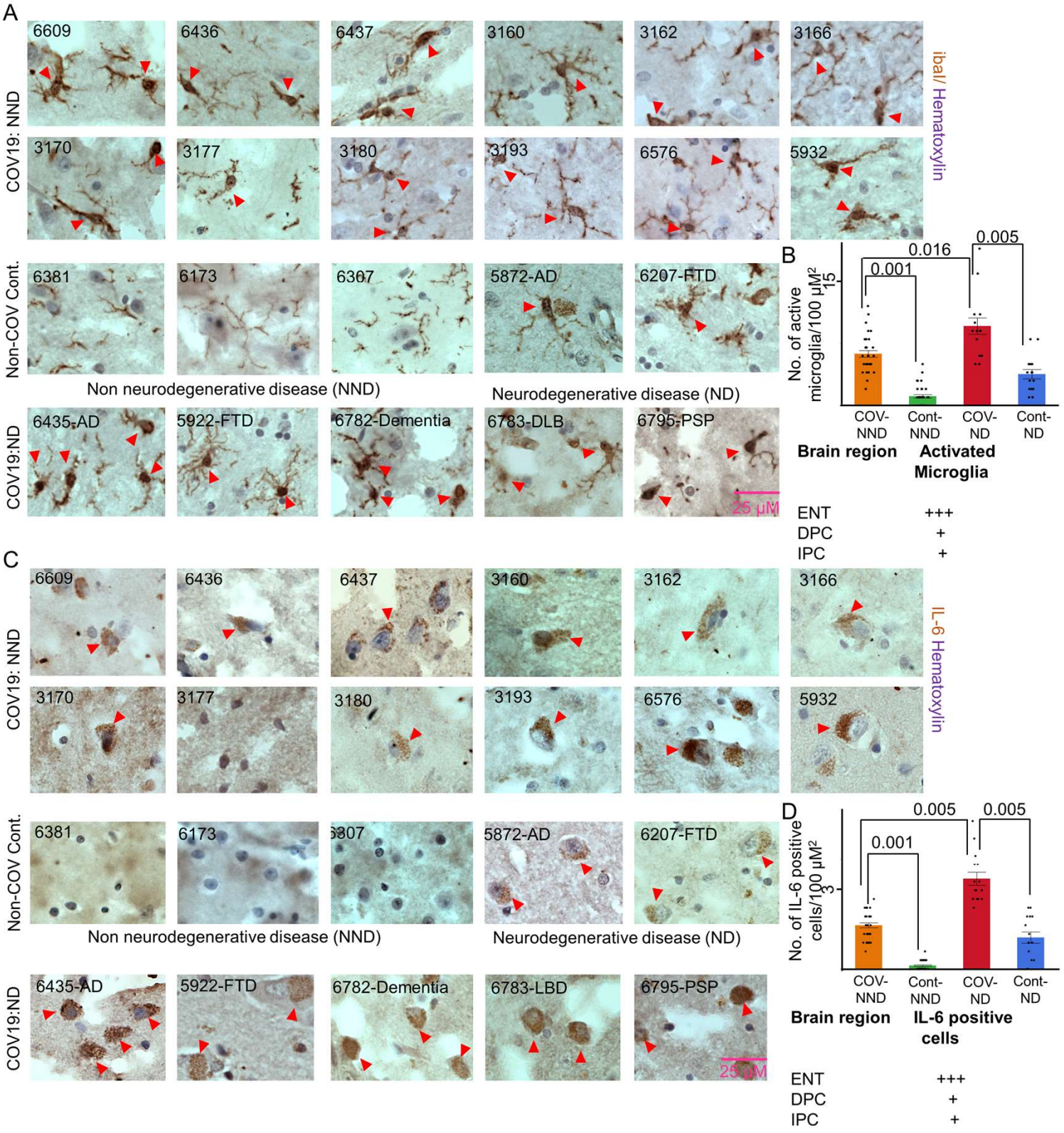

Fig. 5

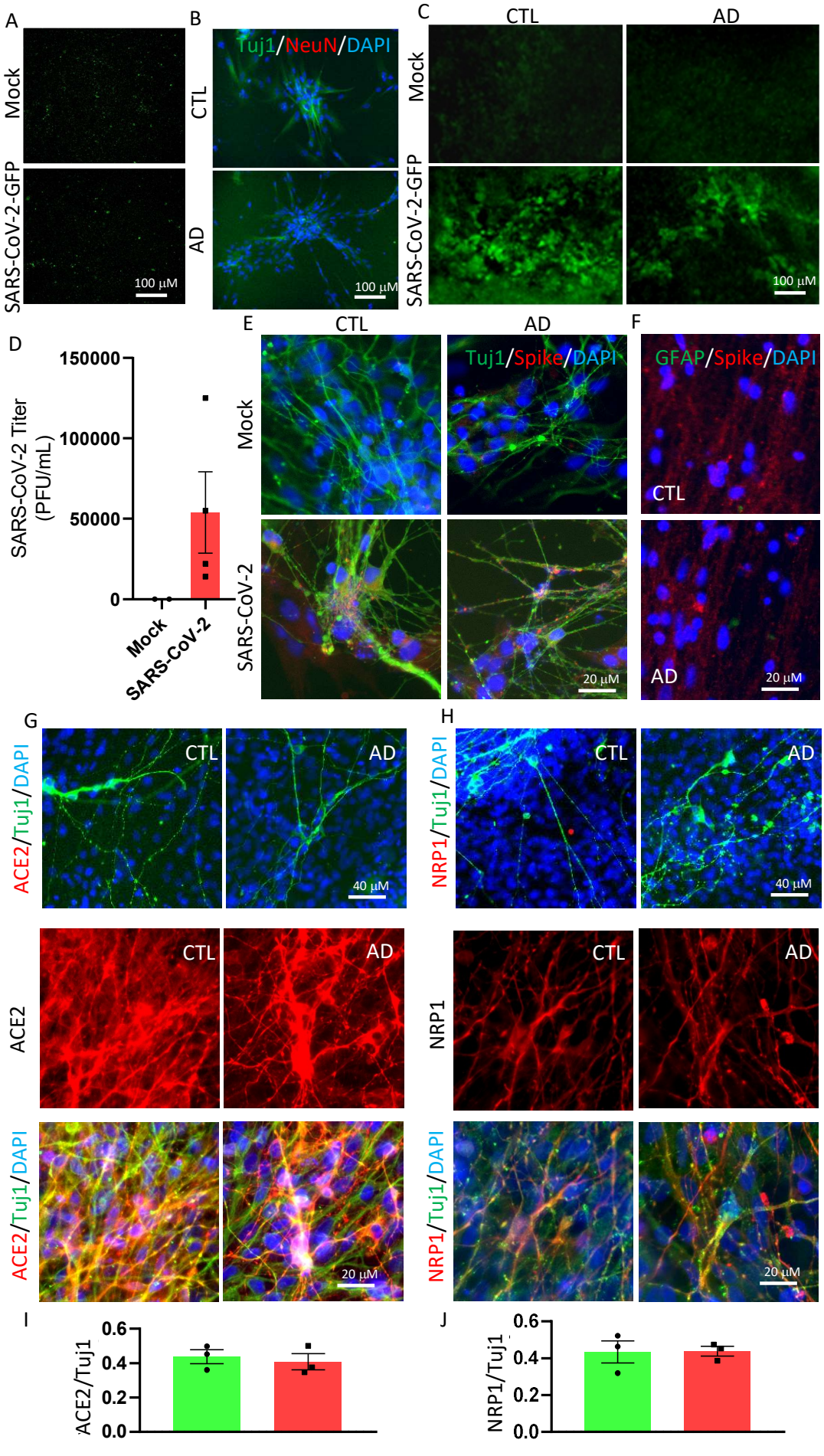

Fig. 6

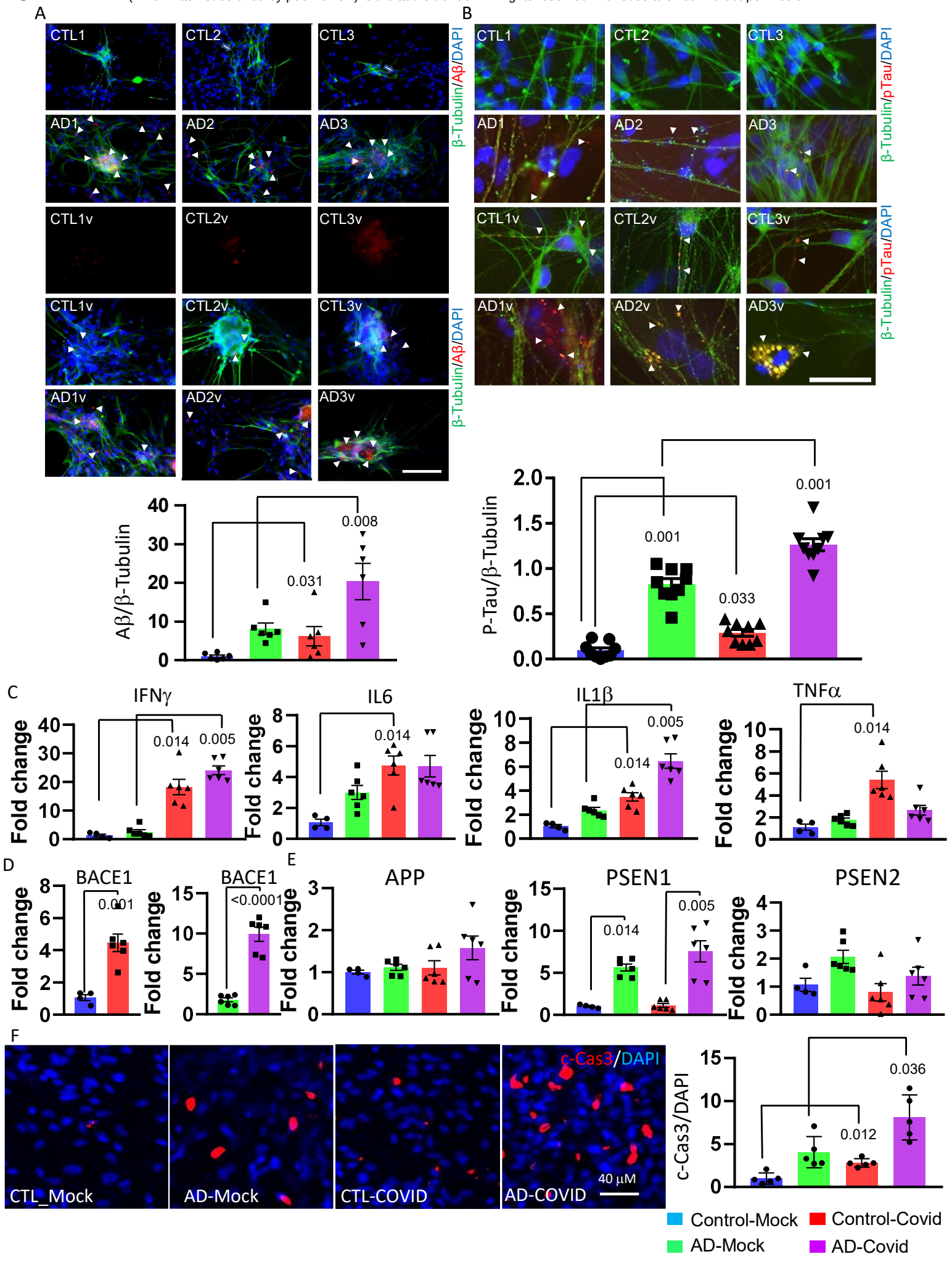

Fig. 7

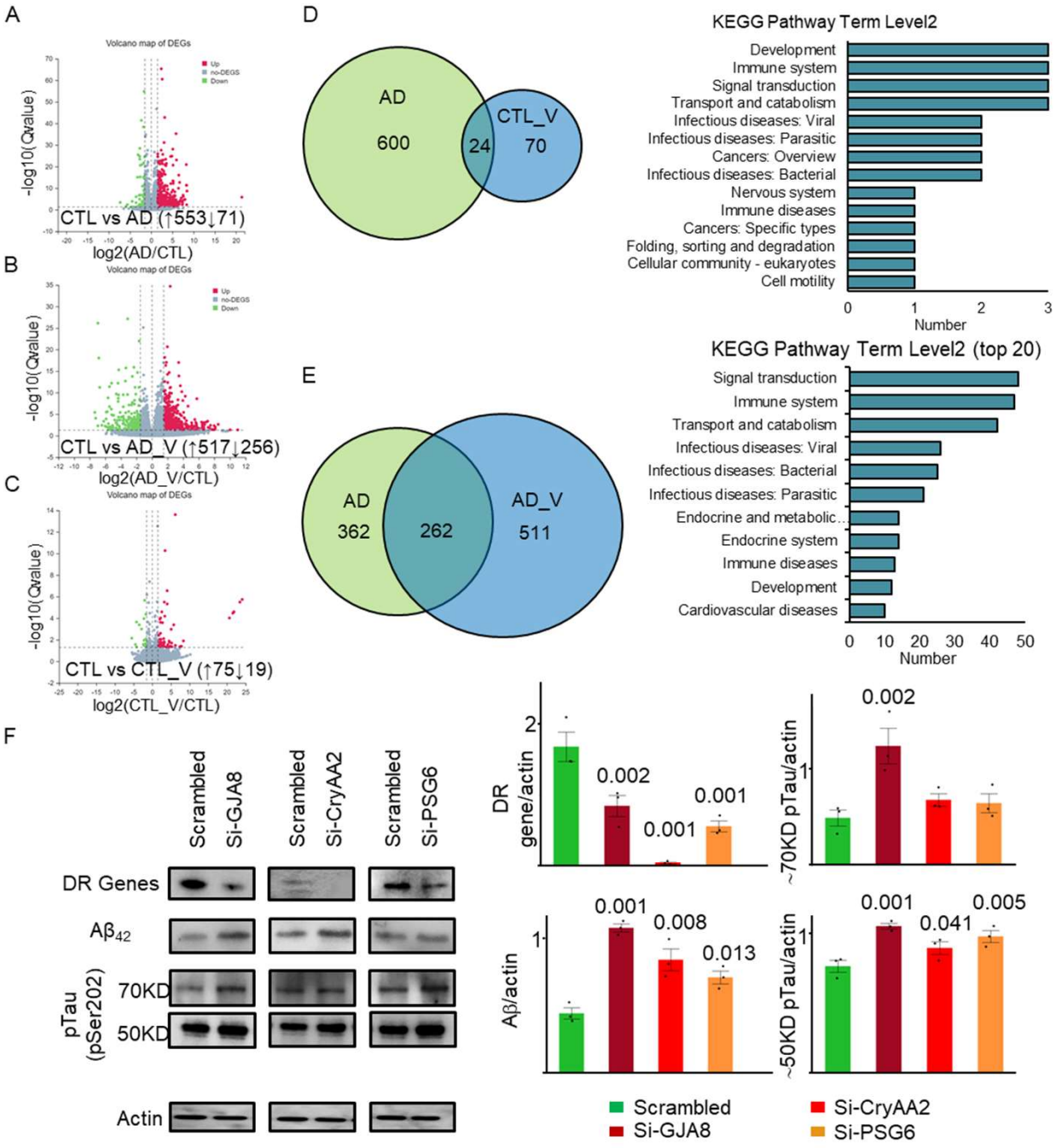

Supplementary Information for

SARS-CoV-2 invades cognitive centers of the brain and induces Alzheimer's-like neuropathology

Wei-Bin Shen, Montasir Elahi, James Logue, Penghua Yang, Lauren Baracco, E. Albert Reece, Bingbing Wang, Ling Li, Thomas G Blanchard, Zhe Han, Robert A Rissman, Matthew B Frieman, Peixin Yang

Supplementary information contains

1. Supplementary Table 1
2. Supplementary figures and figure legends

Supplementary Table 1

Samples of 17 COVID-19 cases and the age-matched non-COVID-19 controls

Case#	Other Dis	Age	Gender	Fixation	Case #	Other Dis	Age	Gender	Fixation
COVID-19 NND					**Non-COV NND**				
6436	ASD	38	F	2020	6381	ASD	30	F	2019
6437	ASD	30	M	2020	6212	ASD	36	M	2018
6576	Seizure	29	M	2021	6274	Healthy	31	M	2019
6609	ASD	31	M	2021	5934	ASD	28	M	2015
3160	ADHD	36.7	M	2021	6062	Healthy	32	F	2017
3162	Healthy	46.4	M	2021	6173	Healthy	49	M	2018
3166	Healthy	25.4	F	2021	6061	Healthy	24	M	2017
3170	MDD	51.6	F	2021	5645	MDD	46	M	2013
3177	Healthy	0.2	M	2021	6307	Healthy	0	F	2020
3180	Healthy	26.9	M	2021	6099	Healthy	30	M	2017
3193	Healthy	18.7	M	2021	6235	Healthy	21	F	2019
5932	Healthy	77	M	2021	6168	Healthy	68	M	2018
COVID-19 ND					**Non-COV ND**				
6782	Dementia	76	F	2021	6632	Dementia	77	F	2021
6783	LBD	78	F	2021	6384	LBD	73	F	2020
6795	PSP	70	M	2021	6225	PSP	87	M	2019
6435	AD	77	M	2020	5872	AD	76	M	2019
5922	FTD	71	F	2020	6207	FTD	73	F	2018

AD: Alzheimer's disease; ADHD: Attention-deficit/hyperactivity disorder; ASD: Autism Spectrum Disorder; FTD: Frontotemporal disorders; LBD: Lewy Body Dementia; MDD: major depressive disorder; PSP: Progressive supranuclear palsy; NND: non-neurodegenerative disease; ND: neurodegenerative disease.

Supplementary figure titles and legends

Supplementary Fig. 1. RS-COV-2 RT PCR and spike protein in the Ent of virus-infected brains.

(**A)** SARS-CoV-2 Spike RNA *in situ* hybridization in the entorhinal cortexes of non-COVID-19 cases. 9 cases of brains without neurodegenerative disease (NND) and 3 cases with neurodegenerative diseases (Dementia, LBD, and PSP). Scale bar 25μM. (**B**). COVID-19 RTPCR revealed COVID-19 positivity in brain regions of three COVID-19 cases along with lung positivity (ID 6436). 72bp band was detected as the target band. Housekeeping gene Actin PCR was carried out to confirm the cDNA input. *the lower band/double band indicated fragmented RNA. (**C**). Representative images of SARS-CoV-2 Spike in the entorhinal cortexes (Ent) of SARS-CoV-2 positive and non-COVID-19 cases. Infected brains without underlying neurodegenerative disease are presented in the upper two panels. The third panel represents the non-COVID-19 control. The fourth panel represents the COVID-19 infected cases with different neurodegenerative diseases. Spike protein staining signals were visualized with a DAB-Nickel, in a reaction of horse radish peroxidase (HRP)-coupled with anti-rabbit secondary antibody (Fab fragments). SARS-CoV-2 spike protein black dot signals were in the cytosol/membrane of the neuronal cells (indicated by red arrows). The brain IDs are presented at the top left. Scale bar 25μM. Spike protein (DAB staining, black dot signals; counterstained with hematoxylin, blue). The graphs show the number of spike protein positive cells per 200 μm^2 (3 independent images for one case) for NND (non-neurodegenerative disease) and ND cases. Data were analyzed by. Graphs are represented as the means ± SEM and were analyzed by the Mann-Whitney U test after confirming the data distribution. and *P*-values indicated in the graphs. **(D)** SARS-CoV-2 nucleocapsid protein (NC) in the entorhinal cortexes of non-COVID-19 cases. 9 cases of brains with no neurodegenerative diseases and 3 cases with underlying neurodegenerative diseases. Scale bar 25μM.

Supplementary Fig. 2. (**A**) Immunofluorescence analysis of MAP2 (Red signals) and hACE2 (Green signals)-positive cells in the Ent of the COVID-19 adult brains (6609, 3193, and 6782). Scale bar 25 μM. (**B**) *In situ* hybridization of SARS-CoV-2 RNA with a NeuN antibody staining showed the presence of the viral RNA in the neurons of the SARS-CoV-2 infected brains Ent (ID: 3170,6576,3160,6782,6535) and Non-COV control (6381). Scale 10 μM. Modification of the *In situ* hybridization method reduced the number of detectable virus particles (red dots). (**C**) Immunofluorescence analysis of Capsid (Red signals) and NeuN (green signals)-positive cells in the Ent of the SARS-CoV-2 infected adults' (3170, 6782,6576) and the infant (3177) brains. Scale bar 25 μM. (**D** Representative images for immunofluorescence analysis of Capsid (Red signals) and Fluro-Jade C (Green signals)-positive cells in the Ent of the SARS-CoV-2 infected NND brains (3166, 6576,6609 and 3193; in the upper panel; Scale bar 50 μM), ND brains (6782,6783,6795) and non-COV ND (6384) brains. The degenerating neurons are indicated (scale bar 25 μM).

Supplementary Fig. 3. (**A**) Aβ immunohistochemical staining in the Ent region of non-COV controls (9 NND and 3 ND cases). Cytoplasmic was amyloid observed only in LBD control (6384). Scale bar 25 μM. (**B**) p-Tau (pSer202) immunostaining in the Ent region of non-COV controls. Intracellular/cytoplasmic deposition of p-Tau (red arrow) and aggregated tau deposit (tangles, astrocytic tau deposition, etc.; yellow arrow) are indicated. Scale bar 25 μM. Tau Tangles are observed in Dementia and astrocytic tau depositions were observed in PSP. (**C**) Immunofluorescence analysis of p-Tau (pSer202; green signal) and SARS-CoV-2 Capsid (red signal) in different SARS-CoV-2 infected brains (3170,6576,6782, and 3166). Scale bar 25 μM.

Supplementary Fig. 4. IL-1β expression in the virus-infected brains.

(**A**) Immunostaining of the microglial marker Iba-I in the Ent region of non-COV controls. Activated

microglia (red arrows) are indicated and the brain IDs are mentioned at the left top of each image. Scale bar 25 μM. (**B**) IL-6 Immunostaining in the Ent region of non-COVID-19 controls. IL-6 positive cells (red arrow) are indicated, and the brain IDs are mentioned at the left top of each image. Scale bar 25 μM. (**C**). Representative images of immunostaining of the cytokines Interleukin-1β (IL-1β) in the Ent region of SARS-CoV-2-infected non-neurodegenerative cases (total 12; upper two panels), non-COVID-19 controls (third panel) and SARS-CoV-2-infected neurodegenerative disease cases (5 different types of neurodegenerative cases; fourth panel). IL-1β positive neurons (red arrow) are indicated. Scale bar 25 μM.

Supplementary Fig. 5. SARS-CoV-2 infects mature neurons derived from human iPSCs.

(**A**) SARS-CoV-2-GFP does not infect immature neurons at iPSC differentiation day 35. White asterisks (*) indicate nonspecific fluorescent signals. (**B**) Immature neurons do not express the mature neuron marker NeuN. (**C**). SARS-CoV-2 infects mature neurons at iPSC differentiation day 50. (**D**). SARS-CoV-2-GFP infects mature neurons at different dosages. CTL (non-AD: iPSCs derived from healthy individuals): control groups; AD: Alzheimer's disease; Tuj1: beta-Tubulin III; SPIKE: SARS-CoV-2 spike protein.

Supplementary Fig. 6. Effects of identified Alzheimer's infectious etiology genes on Aβ and p-Tau in human primary neurons. (**A**). Upregulated genes in AD neurons that were further upregulated due to SARS-CoV-2 infection. (**B**). Downregulated genes in AD neurons that were further downregulated due to SARS-CoV-2. (**C**). KEGG pathway analysis of the upregulated and downregulated genes in AD neurons that were further upregulated and downregulated by SARS-CoV-2. CTL (non-AD: iPSCs derived from healthy individuals): control groups; AD: Alzheimer's disease; ADV: SARS-CoV-2-infected AD group. For each group, n = 3.

(**D**) Immunofluorescence staining with the indicated antibodies after lentivirus-mediated overexpression of the top 3 upregulated genes, FCGR, LILRB5 and OTOR, identified in Fig. 7D as AD infectious etiology genes. Combined or individual overexpression of these three genes did not induce Aβ cellular aggregation, and only FCGR overexpression increased Tau phosphorylation at Ser202.

(**E**) Immunofluorescence staining of the indicated antibodies after siRNA-mediated knockdown of the top 3 downregulated genes, GJA8, CryAA2 and PSG6, identified in Fig. 7D as AD infectious etiology genes. Knockdown of GJA8, CryAA2 or PSG6 individually caused Aβ cellular aggregation and significantly increased Tau phosphorylation at Ser202.

Supplementary Fig. 1.

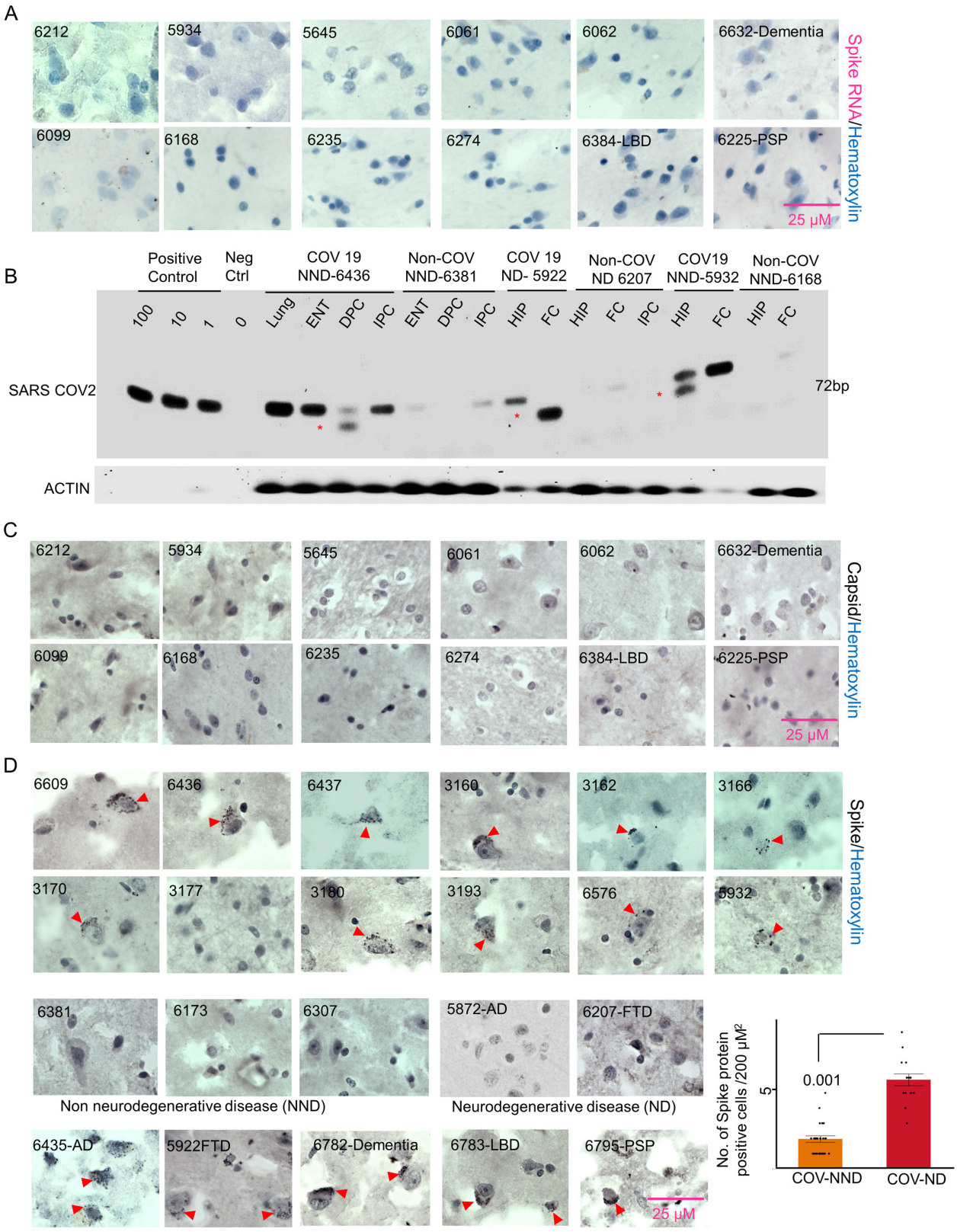

Supplementary Fig. 2.

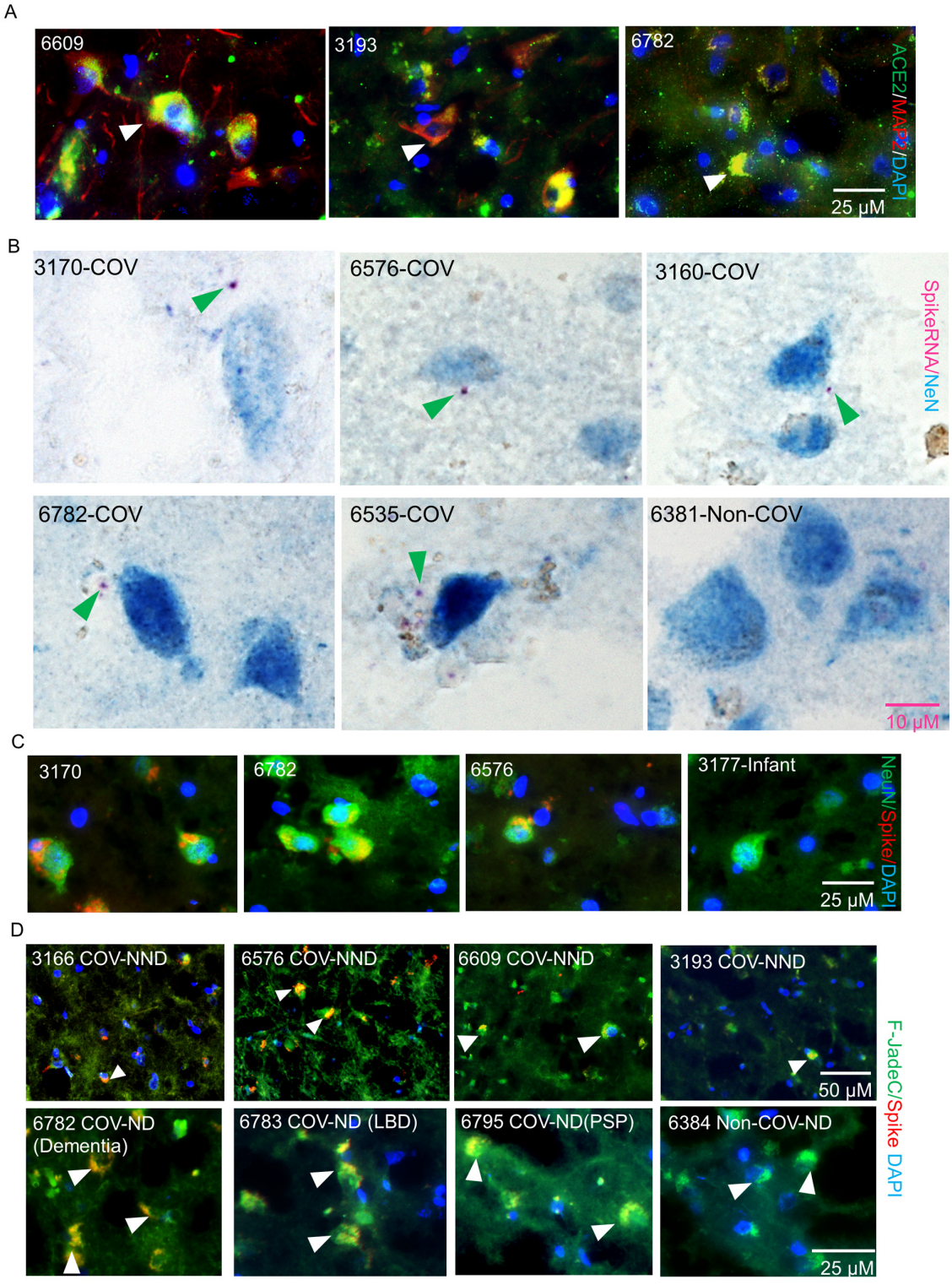

Supplementary Fig. 3.

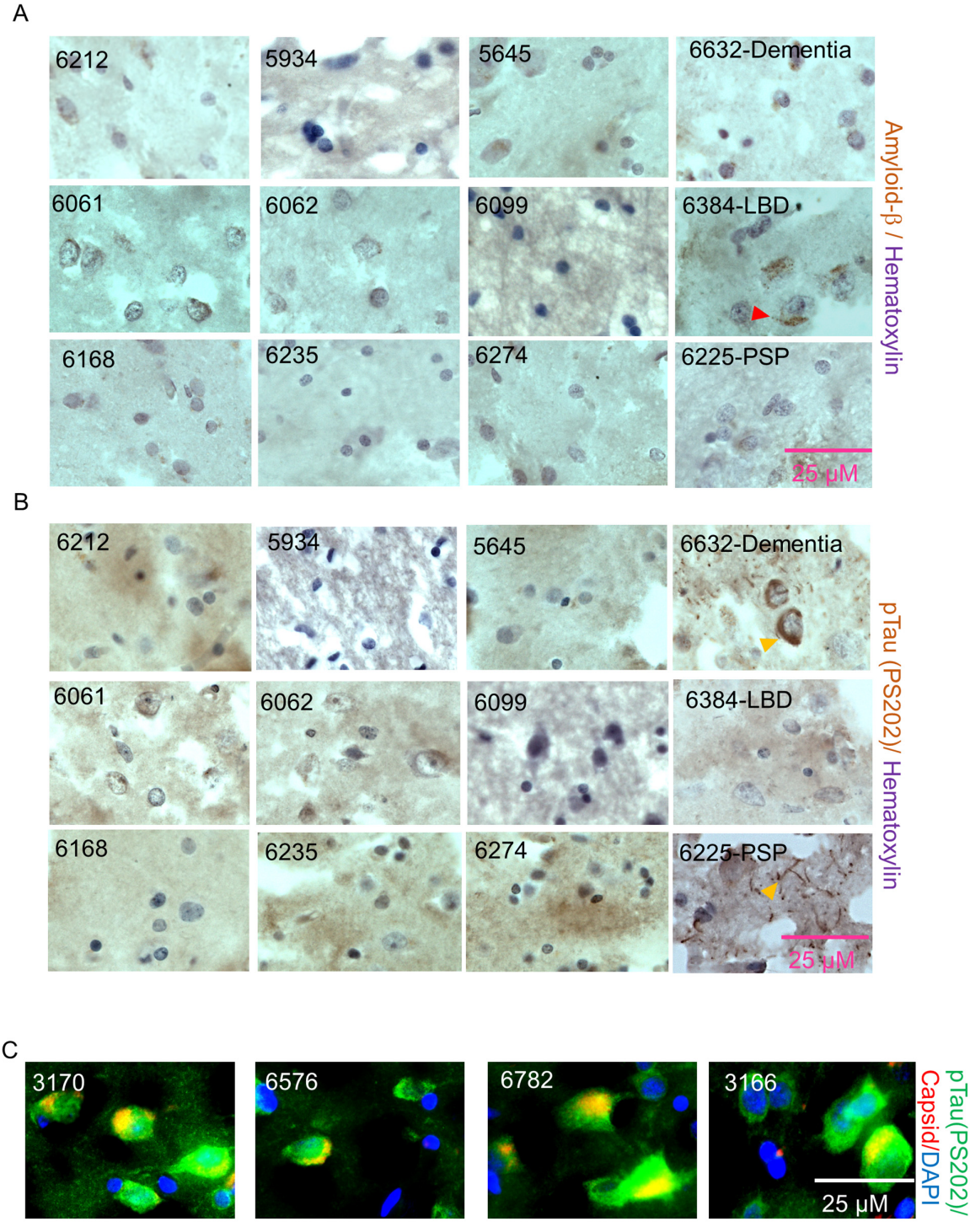

Supplementary Fig. 4.

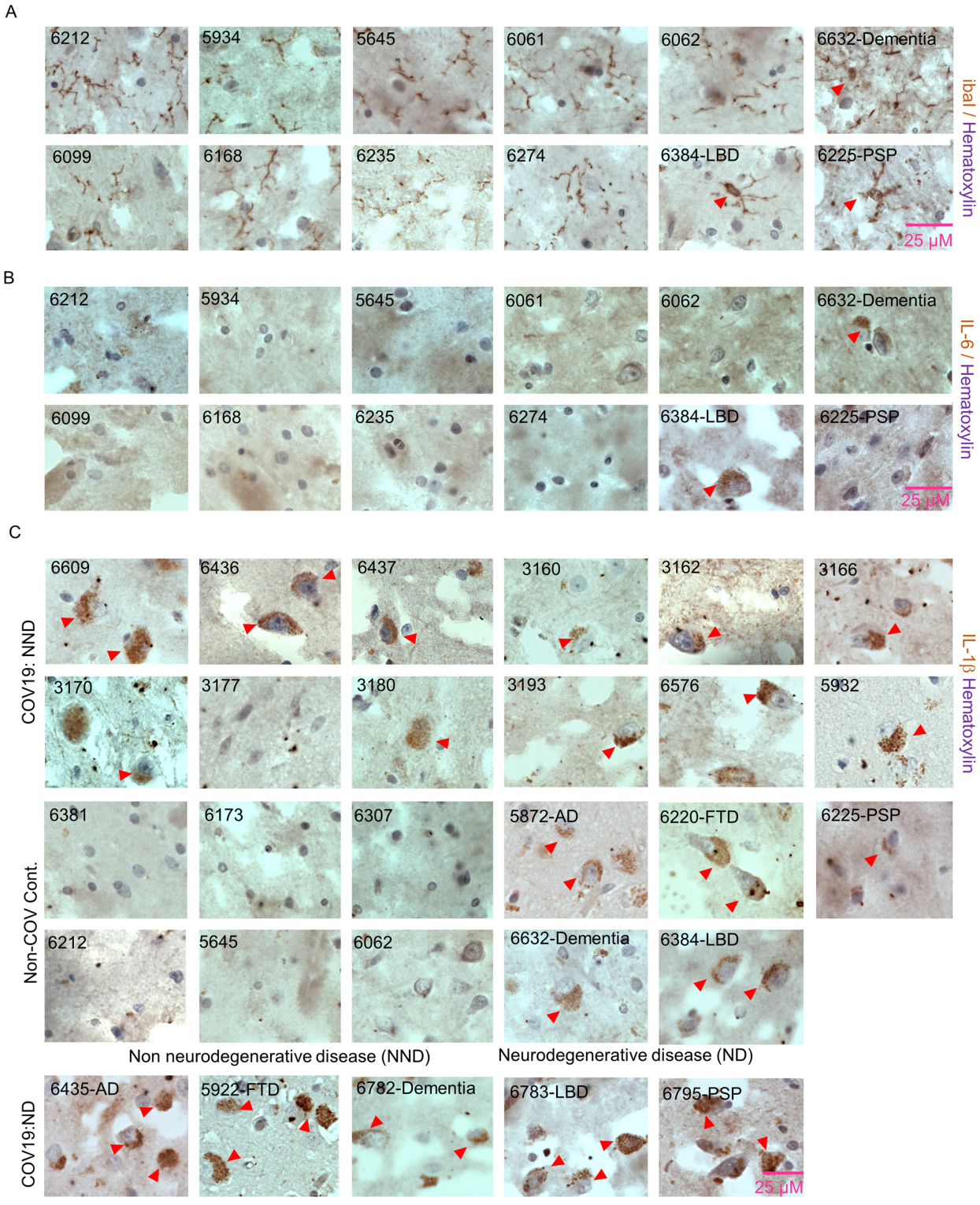

Supplementary Fig. 5.

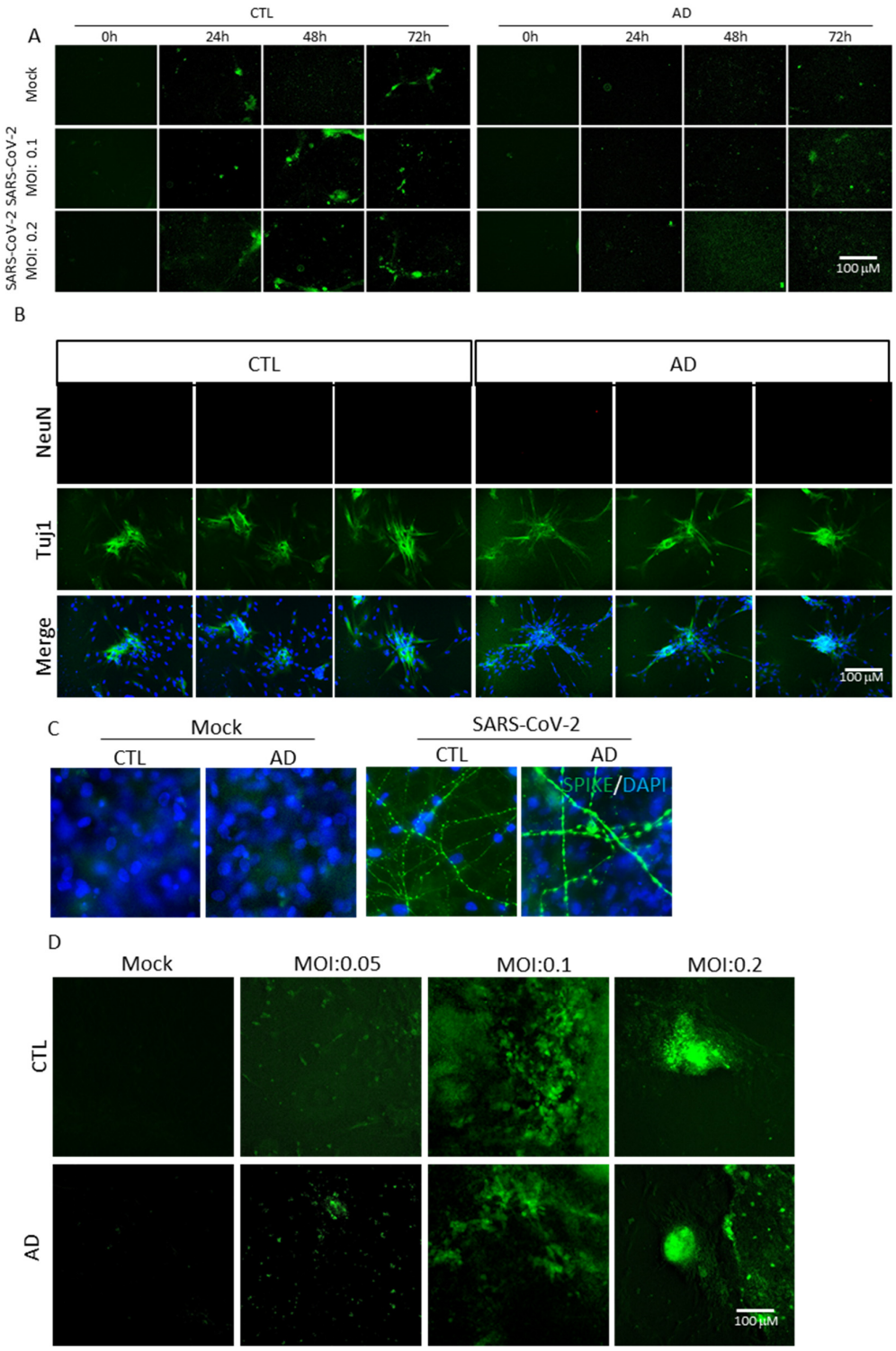

Supplementary Fig. 6.

A

Gene	CTL/AD	CTL/AD_V
XAF1	1.60	3.58
TWIST2	1.81	3.96
CASP4	1.55	3.17
CD34	1.82	3.54
CCL4	2.83	5.49
CCL3	3.40	6.44
KLHDC7B	1.79	3.33
LILRB1	4.37	8.12
GJB2	1.84	3.40
LAIR1	1.92	3.38
PLA2G7	2.08	3.66
C3	2.31	4.05
FIBIN	1.67	2.85
HCK	1.99	3.36
SP140L	1.60	2.68
COMP	1.69	2.83
SLC22A4	1.53	2.53
LRRC25	2.42	3.91
CTSS	2.38	3.78
SLAMF8	2.16	3.36
FERMT3	3.28	5.09
NPL	1.55	2.38
ITGAL	2.83	4.32
AOAH	2.29	3.48
CCL3L1	5.34	8.10

B

Gene	CTL/AD	CTL/AD_V
PLA2G2F	-1.58	-5.46
CRYAA2	-1.88	-5.82
ABCB11	-1.65	-4.64
GJA8	-1.81	-5.06
CRYBB3	-1.76	-4.11
CRYBB1	-2.58	-5.90
C1orf105	-1.65	-3.70
CRYBA1	-2.68	-6.02
MIP	-3.11	-6.95
CRYBA4	-2.58	-5.66
GPD1	-1.60	-3.43
BHMT	-2.52	-5.31
PITX3	-2.07	-4.33
CRYBA2	-3.24	-6.72
GJA3	-1.63	-3.38
CRYGS	-2.73	-5.65
PSG7	-3.39	-6.95
PSG3	-3.17	-6.45
KMO	-1.78	-3.62
PSG2	-3.57	-7.24
CRYGD	-1.83	-3.70
CRYAB	-2.33	-4.53
CRYBB2	-2.84	-5.46
HSD3B1	-1.60	-2.96
PROX1	-1.67	-2.99
VIT	-1.68	-2.99
ERICH5	-1.59	-2.80
AQP5	-1.70	-2.96
PSG1	-2.66	-4.61
COLGALT2	-1.56	-2.61
CRYGC	-2.69	-4.45
ANKRD34C	-2.56	-4.18
DBX2	-2.75	-4.29
MAMDC2	-1.68	-2.54

C

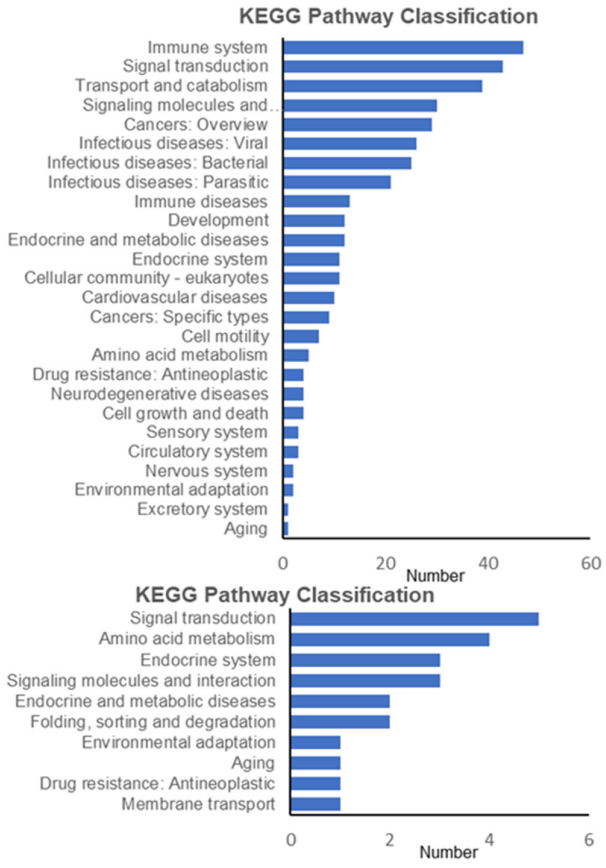

D

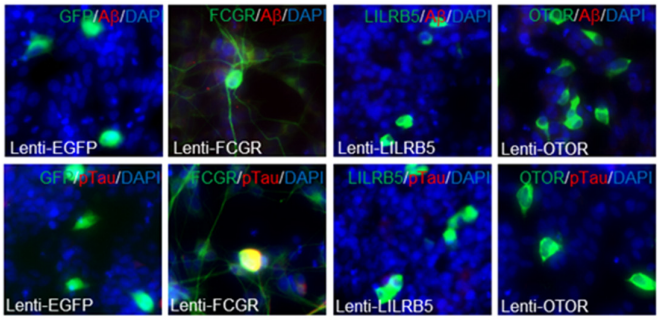

E